

Wage Erosion with Incomplete Markets: A Quantitative Analysis of the Costs of Inflation*

Jafet Baca[†] Andrés Blanco[‡] Andrés Drenik[§]

April 16, 2026

Abstract

In an economy with infrequent nominal wage adjustment, positive trend inflation erodes real wages between adjustment periods. With incomplete financial markets, this erosion amplifies idiosyncratic consumption volatility and reduces household welfare. We quantify this mechanism using monthly administrative labor income data from Argentina under low- and high-trend inflation. We estimate a statistical model of monthly labor income risk that incorporates wage adjustments both within and across jobs, and embed it in a Bewley-Aiyagari model. An increase in trend inflation from 0% to 22% reduces welfare—measured in consumption-equivalent units—by 1.02%.

Keywords: Inflation, Labor Market, Wage Rigidity, Incomplete Markets **JEL Classification:** E12, E31, D31

*The views expressed here are those of the authors and not necessarily those of the Federal Reserve Bank of Atlanta or the Federal Reserve Board.

[†]Emory University. Email: jafet.baca.obando@emory.edu.

[‡]Federal Reserve Bank of Atlanta and Emory University. Email: julioablanco84@gmail.com.

[§]University of Texas at Austin and NBER. Email: andres.drenik@austin.utexas.edu.

1 Introduction

A central question in monetary economics is what inflation target a central bank should pursue. The answer depends on the costs and benefits associated with different levels of inflation—hereafter referred to as trend inflation. In the existing literature, the costs of inflation are linked to several mechanisms: distortions in the demand for fiat money (Baumol, 1952; Friedman, 1969); frictions in nominal price adjustment, such as menu costs and relative price distortions (Blanco, 2020); and the lack of indexation in the tax system (Feldstein, 1976).

In this paper, we propose a new cost of inflation: When nominal wages adjust infrequently, positive trend inflation erodes real wages between adjustment periods. Under incomplete financial markets, this erosion amplifies idiosyncratic consumption volatility and reduces household welfare. The goal of this paper is to quantify the magnitude and welfare implications of this channel.

The first step in our analysis is to document wage adjustments within and across jobs during low- and high-inflation periods. We use monthly administrative employer-employee matched data from Argentina covering both a low-inflation period with 0% annual inflation and a high-inflation period with 22% annual inflation. To assess how inflation affects wage dynamics, we begin with two observations. First, nominal wages can adjust in three situations: (i) within an ongoing job, (ii) following a job-to-job transition, or (iii) after a spell of unemployment leading to reemployment. Second, for economic decision-making, what ultimately matters are changes in real wages, which reflect the gap between lumpy nominal wage adjustments and accumulated inflation. For these reasons, we focus on real wage changes, defined as the nominal wage adjustment net of cumulative inflation since the last nominal wage change—measured both within and across jobs.

In the low-inflation period, the distribution of real wage changes within jobs is characterized by a lack of negative values and a concentration of small, positive changes. Compared to within-job changes, the distribution of real wage changes across jobs is more dispersed: wage changes following job-to-job transitions exhibit a higher mean and a thicker right tail, while those following unemployment spells tend to have a lower mean and a more pronounced left tail.

In the high-inflation period, the distribution of real wage changes within jobs becomes symmetric with a lower mean. Moreover, dispersion increases across all types of real wage changes, accompanied by a decline in the prevalence of small wage adjustments. In this environment, the frequency of within-job wage changes increases.

To link wage erosion to idiosyncratic consumption volatility, we estimate a statistical Markov model of wage adjustment and employment dynamics at a monthly frequency. At any point in time, a worker can

be either employed or unemployed. If employed, the worker receives a nominal wage; if unemployed, income is given by home production in units of consumption. Transitions between employment and unemployment are exogenous and depend on the worker's age and productivity.

Real wages consist of a transitory and a permanent component. The permanent component erodes with inflation between adjustments and is reset to a target composed of two elements: a worker-specific component and a match-specific component. The worker-specific component follows a random walk, with a drift that depends on the worker's employment status. The match-specific component is constant within a match and resets upon a job transition. The probability of adjustment within a match depends on the gap between the reset wage and the current (eroded) wage. Job-to-job transitions are exogenous and also depend on the worker's age and productivity.

We estimate the model using the method of simulated moments (SMM) under the low-inflation regime, targeting the empirical distributions of wage changes within and across jobs, as well as key labor market indicators such as job separations, job-to-job transitions, and lifecycle income statistics, including the cross-sectional mean of monthly income by age. The model closely replicates the observed wage change distributions and lifecycle income profiles under low inflation. For the high-inflation regime, we re-estimate only the subset of parameters governing within-job wage changes, targeting their empirical counterparts.

To quantify the welfare cost of inflation, we then embed our empirically estimated labor income process into a Bewley-Aiyagari dynamic consumption-savings model. In this framework, a continuum of heterogeneous workers in a small open economy make consumption and saving decisions to maximize expected lifetime utility, subject to a no-borrowing constraint and a liquid risk-free bond. The *real* rate of return of this bond is negative, making it costly for workers to save away anticipated shocks. Workers face idiosyncratic labor income risk, which evolves according to the stochastic process we estimate from the data. This process incorporates a positive reset wage to equalize the average real wages across inflation regimes. This allows us to focus on how inflation affects wage erosion (instead of conflating these effects with differences in the mean level of real wages) and assess how inflation-induced wage erosion and income risk jointly affect household welfare.

Under the baseline calibration of the model, we calculate a consumption equivalent variation of 1.02%. That is, on average, households would need to increase their consumption by 1.02% each month in the high-inflation regime to be indifferent to living in a low-inflation economy. This result reflects the interplay of several economic forces. On the one hand, if the frequency of wage changes does not respond to inflation, higher inflation increases the variance of real income during employment, thereby raising the cost of inflation. On the other hand, when the frequency of wage changes increases with inflation,

this partially offsets the above effect and introduces a benefit: contractual wages adjust more frequently, leading to thinner tails in the distribution of within-job wage changes. Additionally, we find that the welfare cost of inflation is larger for high-income workers for two main reasons: (i) lower-income workers spend more time unemployed and rely more on home production income, which is fixed in real terms and unaffected by inflation; and (ii) higher-income workers are less likely to switch jobs and therefore less likely to reset their contractual wages, making them more vulnerable to real wage erosion.

We perform several checks to gauge the robustness of our main result. First, we populate the economy with hand-to-mouth workers. We find that the consumption equivalent increases to 2.04%. Thus, our result is robust to varying degrees of market incompleteness. Given that inflation could in addition reduce the real rate of return of liquid assets, we perform an additional exercise in which we decrease the real rate of return of liquid assets and obtain an average consumption-equivalent welfare loss of 2.92%. Finally, we perform an additional exercise in which we equalize the reset wage across inflation regimes, which causes the average real wage in the low inflation period to be greater than its high inflation counterpart. In this exercise, the consumption-equivalent welfare cost increases substantially to 7.68%.

Related Literature. This paper builds on the seminal contribution of [İmrohoroğlu \(1992\)](#), who studies the welfare costs of inflation in a Bewley model where agents can save only in fiat money and real income is independent of trend inflation. In her framework, money demand is mainly driven by precautionary savings. As inflation erodes the value of money holdings, household welfare decreases. Specifically, a 10% increase in inflation lowers welfare by approximately 1% in consumption-equivalent terms. [Allais et al. \(2020\)](#) extend this framework by incorporating both real and nominal assets, while [Erosa and Ventura \(2002\)](#) introduce transactional motives for holding money. A common feature of these models—and those described above—is that the welfare cost of inflation tends to be approximately quadratic and relatively small for moderate levels of trend inflation. Our contribution departs from this literature by allowing for the possibility that real labor income varies with inflation. We document this relationship empirically and quantify its implications using a standard Bewley-Aiyagari model augmented with nominal wage rigidity and labor market frictions. We abstract from the effects of inflation on markdowns and productivity, leaving these for future research.

2 Wage Adjustment Across Inflation Regimes

This section documents wage-setting behavior across different levels of trend inflation, which is at the core of our theory of the cost of inflation developed in the next sections. We begin by describing the data

and the construction of our measure of realized and contractual wages (i.e., the permanent component of realized wages). We then present our findings on the distribution of *real* wage changes and the frequency of changes across two inflation regimes.

2.1 Data

Data description. We use an anonymized, publicly available version of administrative employer-employee-matched monthly panel data from Argentina, covering the period from January 1996 to December 2021. Our data source is Argentina’s National Social Security System (“Sistema Integrado Previsional Argentino,” henceforth SIPA). SIPA records each worker’s total monthly labor income in the formal sector, including all forms of compensation that may trigger tax liabilities or social security contributions (see Table A1 in the Online Appendix). We refer to total labor income as the nominal wage.

These data cover a random sample of workers and provide unique worker identifiers that are consistent across the entire period, together with firm identifiers that allow us to track labor mobility across firms, although not all workers in a given firm are observed.¹ The dataset also includes relevant demographic information on each worker and their job, as well as some characteristics of the firm, such as its 4-digit industry classification and geographic location (state).

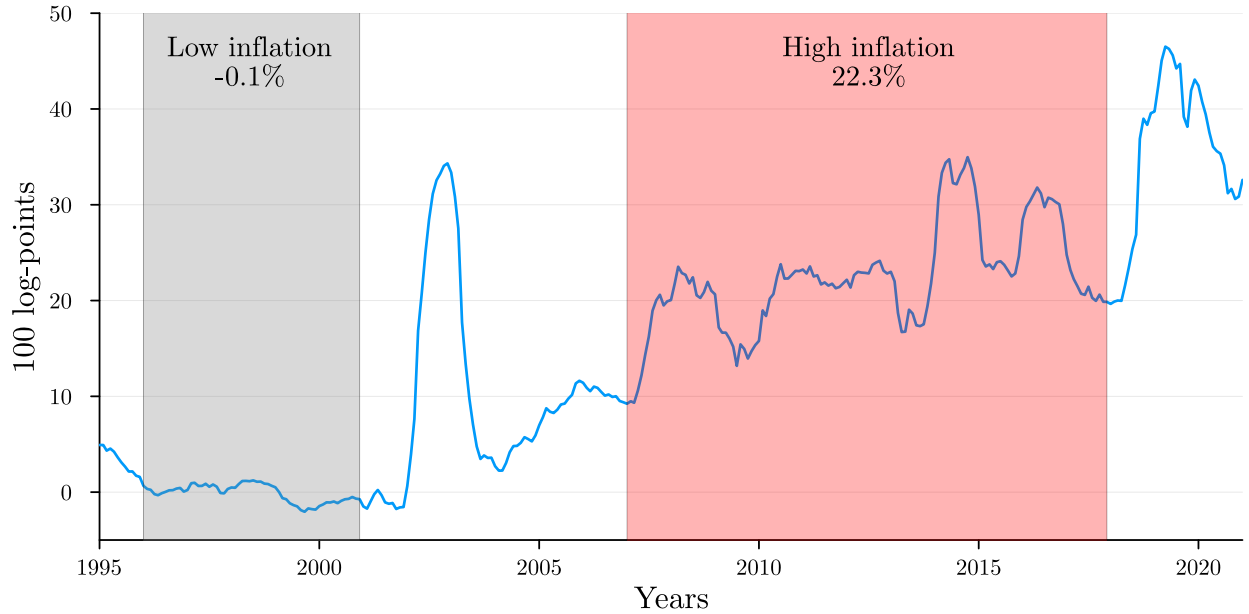
We restrict our sample to male workers aged 25 to 60 to avoid confounding factors related to labor force participation and retirement. We exclude job spells in the public sector, as those wages may not be market-determined and could be influenced by non-market forces. In addition, we remove outliers, defined as workers earning less than half the monthly minimum wage.

Inflation and macroeconomic context. As shown in Figure 1, our sample period spans two distinct inflation regimes. The first, from January 1996 to December 2000, was marked by a fixed exchange rate and a low inflation rate. The second, from January 2007 to December 2017, was characterized by persistently high inflation, driven by structural fiscal deficits, monetary financing of government spending, and repeated currency crises. The average annual inflation rate during the first regime was 0% and 22% during the second regime.²

¹For more details on the data, see [Blanco *et al.* \(2025\)](#). In that paper, the authors validate most of their findings using the full dataset, which is not currently available.

²According to data from the Center of Distributive, Labor and Social Studies (CEDLAS), the labor market composition shifted slightly between these periods, with the informality rate falling from 42.8% to 39.4% and the self-employment rate declining from 21.5% to 19.0% of total workers. Because these modest shifts may have been driven by factors other than inflation, we abstract from them and focus instead on the wage-erosion channel.

FIGURE 1. ANNUAL INFLATION



Notes: The figure shows log annualized inflation at a monthly frequency from January 1996 to December 2021. The shaded gray area highlights the low-inflation period (1996M1-2000M12), with an average inflation rate of -0.1%. The shaded red area highlights the high-inflation period (2007M1-2017M12), with an average inflation rate of 22.3%. Due to the manipulation of inflation statistics in Argentina in 2007, we use consumer price indices provided by national statistics before 2007 and data from PriceStats from 2007 to 2018.

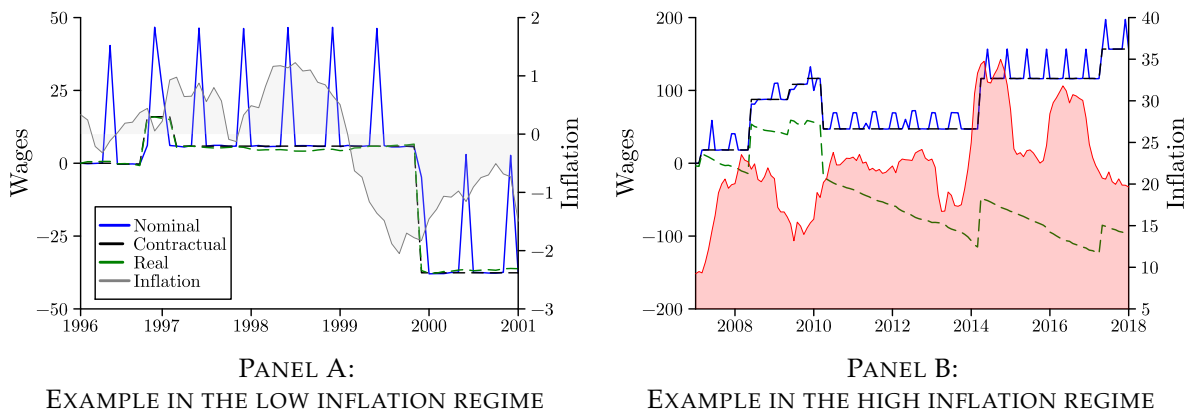
Source: PriceStats and the National Institute of Statistics and Census of Argentina.

Contractual wages. While ongoing employment relationships are characterized by considerable wage rigidity, this rigidity does not extend to hours worked or other transitory earnings components. As a result, observed wages can fluctuate significantly over time around a persistent component. For example, [Ganong *et al.* \(2024\)](#) show that in the United States, while only 10% of workers experience a change in their monthly contractual wage, 69% of them see changes in their total monthly labor income. Since the objective of this paper is to measure the interaction between nominal wage rigidity and inflation, we follow [Blanco *et al.* \(2024\)](#) to recover a measure of the contractual wage.

We first motivate our procedure to recover contractual wages with an illustration. Figure 2 shows the evolution of nominal wages (solid blue line) for two workers in our data. As the figure shows, there are two types of transitory deviations from the contractual wage: (i) significant and seasonal increases in nominal wages of around half the monthly wage, and (ii) small and temporary fluctuations around a modal value. The first type of deviation is mandated by law and reflects the 13th-month salary paid in June and December—a feature not unique to the Argentine economy and common in many Latin American countries. The second type results from a combination of factors, including the intensive margin of labor supply, small bonuses, commissions, and other temporary changes in earnings.

To recover the contractual wage from the data, we use the Kolmogorov-Smirnov test, which allows us to detect the persistent component in non-Gaussian statistical models. Intuitively, the idea is to split a worker’s wage series into two contiguous sub-samples and test whether they are drawn from the same distribution. To do so, the algorithm relies on a single parameter that determines whether the difference between sub-samples is large enough to reject the null hypothesis of no structural break. We set this parameter to 0.56, an intermediate number between the values used in [Stevens \(2020\)](#) (0.60) and [Blanco et al. \(2024\)](#) (0.45).

FIGURE 2. NOMINAL, CONTRACTUAL, AND REAL WAGES FOR TWO WORKERS



Notes: The figure shows the evolution of nominal, contractual, and real wages for two different workers in our data. Panels A and B show a worker’s wage dynamics during the low- and high-inflation periods, respectively. The solid blue line shows the normalized nominal wage. The dark dashed line shows the normalized contractual wage, identified using the Kolmogorov-Smirnov test. The green dashed line shows the normalized real contractual wage, deflated using CPI inflation. The left y-axis displays the three types of wages, while the right y-axis shows annual inflation. All variables are plotted on a $100 \times \log$ scale.

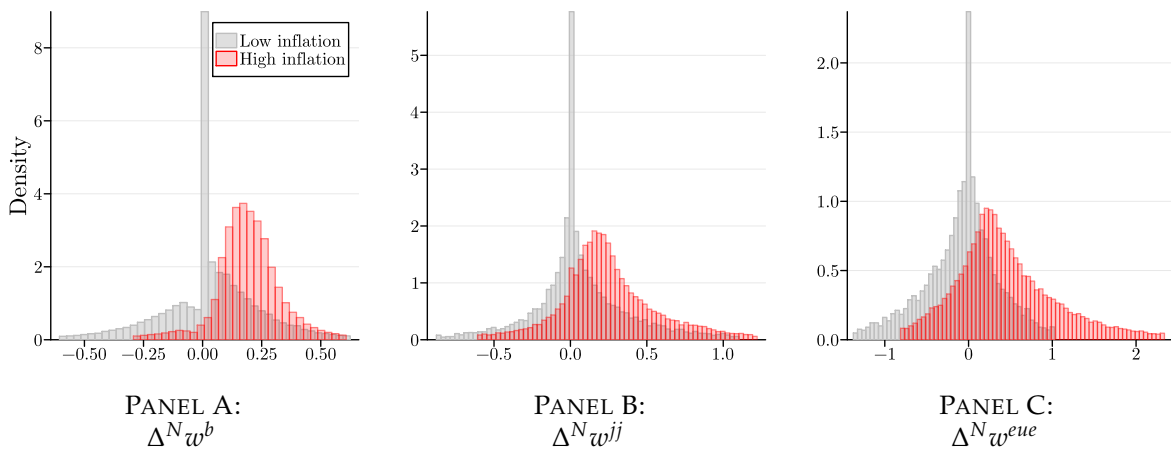
2.2 Wage Changes Across Inflation Regimes

There are three instances in which a worker’s contractual wage can change: (i) during an ongoing job spell, (ii) when a worker is hired from another firm, and (iii) when a worker finds a new job following a period of unemployment. From a theoretical perspective, different frictions may affect each type of wage adjustment differently, and thus lead to distinct statistical properties which could vary with inflation. As [Blanco et al. \(2024\)](#) show, if layoffs are more prevalent than quits to unemployment, we should observe more wage decreases between the old and new jobs following an unemployment spell than within jobs or following direct job-to-job transitions. Alternatively, [Afrouzi et al. \(2026\)](#) show that wage changes of workers poached by other firms respond more strongly than those of job-stayers following an increase in inflation, since they result from different worker decisions.

For those reasons, inflation is likely to interact differently across these types of wage adjustments—an effect we will incorporate in our model. Accordingly, we define and measure three types of (log) nominal contractual wage changes: those (i) within an ongoing job spell, $\Delta^N w^b$; (ii) following job-to-job transitions, $\Delta^N w^{jj}$; and (iii) following an unemployment spell in between consecutive jobs, $\Delta^N w^{eue}$, defined as the difference between the first contractual wage in the new job and the last contractual wage in the previous job. Next, we analyze the size and frequency of these adjustments.

Distribution of nominal and real wage changes. Figure 3 shows the distribution of these non-zero nominal wage changes across different instances of wage adjustments, separately for low- and high-inflation regimes. We begin with the low-inflation period. The first notable feature is the asymmetry of the distributions. The distribution of wage changes within the same job spell is concentrated just above zero, indicating that most workers experience small nominal wage increases, with a mean of around 2%. In contrast, wage changes following job-to-job transitions without an intervening unemployment spell are more symmetric, with a mean of 5%, and roughly 60% of observations showing wage increases. This suggests that workers who change jobs tend to receive larger wage increases than those who stay. Lastly, transitions involving an intervening unemployment spell are skewed toward negative changes: over 50% of changes are wage reductions and the average is approximately -10%.

FIGURE 3. NON-ZERO NOMINAL WAGE CHANGES WITHIN AND ACROSS JOBS



Notes: The figure shows the densities of non-zero nominal wage changes within job spells (Panel A, denoted by $\Delta^N w^b$), following job-to-job transitions without intervening unemployment spells (Panel B, denoted by $\Delta^N w^{jj}$), and following job-to-job transitions with at least one month of unemployment in between jobs (Panel C, denoted by $\Delta^N w^{eue}$). The gray bars show densities for the low-inflation regime, and the red bars represent the densities during the high-inflation regime. All non-zero changes are plotted on a $100 \times \log$ scale. For these plots, we truncate each distribution at the 2nd and 98th percentiles.

Source: Data from SIPA.

Figure 3 also illustrates the distributions during the high-inflation period. The key observation is that, under high inflation, not only do the means change, but the *entire* shapes of the distributions shift. Table 1 quantifies the change in the distributions of nominal wage changes. To mitigate the influence of outliers, we report their dispersion (interquartile range, $P75 - P25$), tail asymmetry (Kelly skewness, $(P90 + P10 - 2P50)/(P90 - P10)$), tailedness/peakedness (Crow-Siddiqui kurtosis, $(P97.5 - P2.5)/(P75 - P25)$), and key percentiles. Nominal wage adjustments become more dispersed after a worker switches jobs or experiences an unemployment spell, while the dispersion of adjustments within jobs remains relatively stable. While the asymmetry of within-job and job-to-job wage changes does not change, wage changes following unemployment spells become positively skewed, which is also illustrated in Figure 3. All three types of wage adjustments exhibit lower kurtosis in the high-inflation regime, indicating that their distributions have lighter tails compared to the low-inflation episode.

To meaningfully compare wage changes across regimes, we convert nominal wage changes to real wage changes, since in economic decision-making, real—not nominal—wages matter. We define real wage changes as the nominal wage change net of the cumulative inflation experienced since the previous nominal wage adjustment. More specifically, let t denote the month of a wage change within a job or the initial month of employment, and let $T(t)$ be the month of the subsequent wage adjustment within a job, or the initial month of employment at a new job. Let $\pi_{T(t),t}$ denote the cumulative inflation between $T(t)$ and t . Then, real wage changes are defined as:

$$\begin{aligned}\Delta^R w_t^b &\equiv \Delta^N w_t^b - \pi_{T(t),t}, \\ \Delta^R w_t^{jj} &\equiv \Delta^N w_t^{jj} - \pi_{T(t),t}, \\ \Delta^R w_t^{eue} &\equiv \Delta^N w_t^{eue} - \pi_{T(t),t}.\end{aligned}$$

Next, we focus on the distribution of these variables conditional on a non-zero nominal wage change (i.e., when $\Delta^N w_t^b$, $\Delta^N w_t^{jj}$, or $\Delta^N w_t^{eue}$ are non-zero). We illustrate the construction of these variables using Figure 2, Panel B. A worker receives a nominal wage increase in April 2014, with the previous adjustment occurring in April 2010, both within the same firm. The nominal wage change is defined as the log difference in contractual wages, while the real wage change is computed by subtracting the cumulative inflation between April 2010 and April 2014. The same logic applies to job transitions, even when the two dates correspond to two different employers.

Figure 4 displays the distribution of real wage changes, restricting the sample to worker-months with non-zero nominal wage changes. Panel A of Figure 4 shows the distribution of real wage changes within jobs. In the high-inflation period, the mass of the distribution shifts from the positive to the negative

TABLE 1. SUMMARY STATISTICS OF DISTRIBUTION OF NOMINAL WAGE CHANGES

	$\Delta^N w$		$\Delta^N w^b$		$\Delta^N w^{jj}$		$\Delta^N w^{eue}$	
	Low	High	Low	High	Low	High	Low	High
Interquartile range	20.86	22.52	19.54	20.34	29.09	35.38	48.49	72.70
Kelly skewness	0.04	0.11	0.02	0.04	0.20	0.20	-0.11	0.22
Crow-Siddiqui kurtosis	5.92	4.90	5.40	4.38	6.07	4.72	4.53	3.98
Frequency	4.72	9.97	4.16	9.29	1.38	1.32	3.99	2.69
Percentiles								
P2.5	-59.11	-30.18	-48.98	-27.22	-74.50	-52.58	-122.76	-72.00
P25	-9.54	4.01	-9.31	3.15	-8.42	6.10	-31.83	5.06
P50	0.24	14.65	-0.05	13.13	1.66	20.82	-2.63	34.68
P75	11.31	26.52	10.23	23.49	20.68	41.48	16.66	77.76
P97.5	64.26	80.17	56.45	61.80	100.82	113.58	96.71	218.04

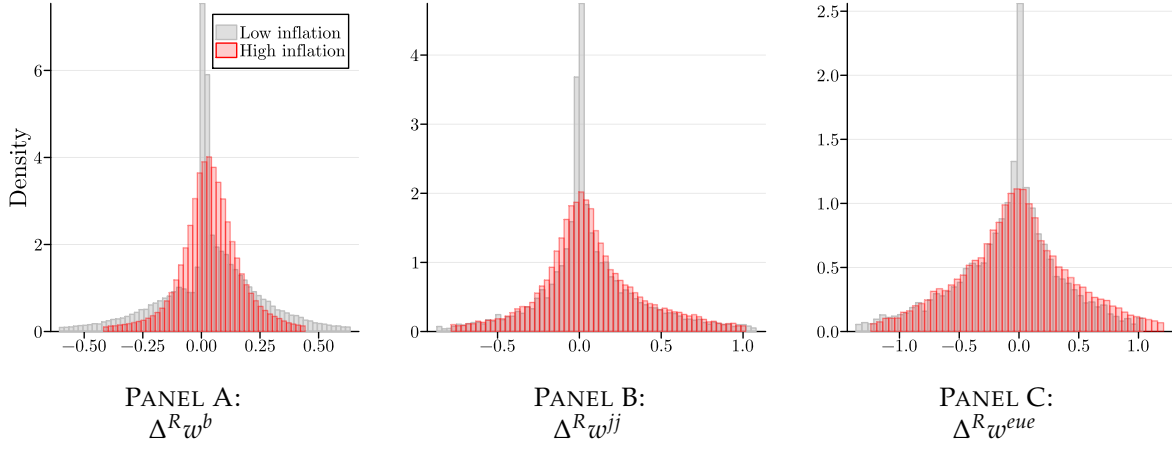
Notes: The table reports summary statistics for the distribution of nominal wage changes during low- and high-inflation periods. The first two columns comprise the entire distribution (excluding nil adjustments). Subsequent columns dissect non-zero wage changes occurring within and across jobs. All statistics are computed based on the original distributions, without truncation. The frequencies reported for changes within a job, job-to-job, and after a job separation represent the respective probabilities of each type of transition.

region—a pattern first documented by [Blanco et al. \(2022\)](#). As shown in Panels B and C, real wage changes following job transitions—both with and without intervening unemployment spells—are more positive under high inflation.

We study the dynamics of higher moments of the distribution of real wage changes in [Table 2](#) and [Figure 5](#). Three key patterns emerge. First, all distributions of real wage changes become more dispersed, especially wage changes following unemployment spells, which exceed 100 log points in spread. The volatility of real wage adjustments increases in the transition period into the high-inflation regime and stabilizes thereafter. Second, under low inflation, wage changes within job spells and following job-to-job transitions exhibit positive skewness, while wage changes after unemployment show negative skewness. Under high inflation, there is a convergence toward symmetry in the tails for both within-job changes and those following unemployment (see [Panel C](#)). Finally, the prevalence of small wage changes across all types of wage transitions disappears under high inflation, as reflected by a sharp decline in the Crow-Siddiqui kurtosis.

Frequency of wage changes. High inflation affects both the size of real wage changes and the frequency of wage adjustments across different employment flows. [Figure 6](#) shows the frequency of wage changes within jobs, following job-to-job transitions, and after job separations. For each type of adjustment, we

FIGURE 4. REAL WAGE CHANGES WITHIN AND ACROSS JOBS



Notes: The figure shows the densities of real wage changes within job spells (Panel A, denoted by $\Delta^R w^b$), following job-to-job transitions without intervening unemployment spells (Panel B, denoted by $\Delta^R w^{jj}$), and following job-to-job transitions with at least one month of unemployment in between jobs (Panel C, denoted by $\Delta^R w^{eue}$). The gray bars show densities for the low-inflation regime, and the red bars represent the densities during the high-inflation regime. Real wage changes are computed in months with a non-zero nominal change. All wage changes are plotted on a $100 \times \log$ scale. For these plots, we truncate each distribution at the 2nd and 98th percentiles.

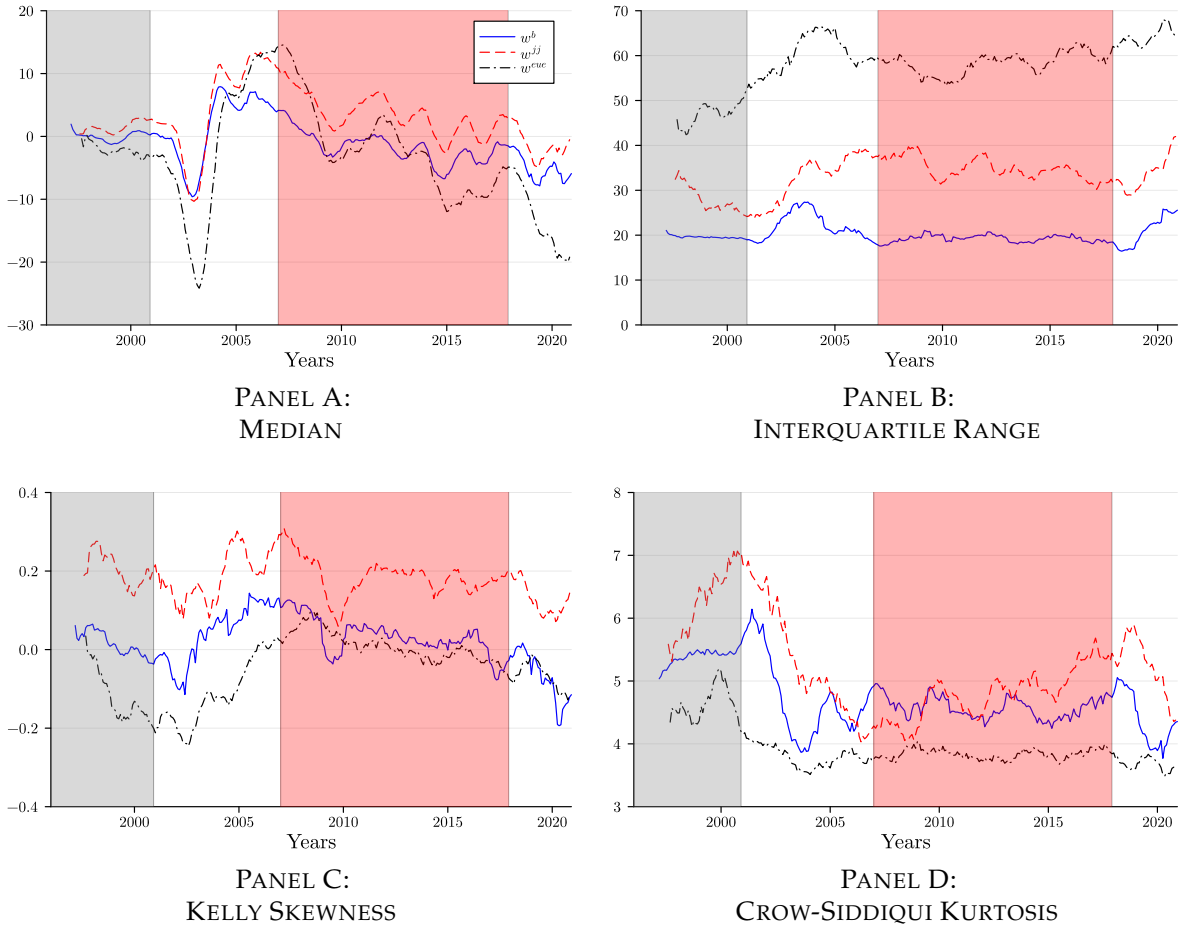
Source: Data from SIPA.

TABLE 2. SUMMARY STATISTICS OF DISTRIBUTION OF REAL WAGE CHANGES

	$\Delta^R w$		$\Delta^R w^b$		$\Delta^R w^{jj}$		$\Delta^R w^{eue}$	
	Low	High	Low	High	Low	High	Low	High
Interquartile range	20.84	20.78	19.59	19.21	27.91	34.80	47.16	58.35
Kelly skewness	0.04	0.06	0.02	0.03	0.21	0.19	-0.12	0.01
Crow-Siddiqui kurtosis	5.92	5.03	5.39	4.58	6.29	4.80	4.63	3.83
Percentiles								
P2.5	-59.04	-48.48	-49.04	-42.13	-73.98	-70.73	-122.12	-111.88
P25	-9.49	-10.92	-9.28	-11.15	-7.94	-10.73	-30.98	-31.62
P50	0.31	-0.74	-0.01	-1.69	1.50	3.52	-2.15	-1.82
P75	11.35	9.87	10.31	8.05	19.97	24.07	16.18	26.74
P97.5	64.26	55.89	56.51	45.73	100.21	95.34	96.25	111.78

Notes: The table reports summary statistics for the distribution of real wage adjustments during low- and high-inflation periods. The first two columns comprise the entire distribution (excluding nil adjustments). Real wage changes $\Delta^R w$ are calculated as nominal wage growth net of contemporaneous inflation. Subsequent columns dissect non-zero real wage changes occurring within and across jobs. Real wage changes following labor transitions are defined as nominal wage growth net of cumulative inflation since the previous wage adjustment. All statistics are computed from the non-truncated distributions.

FIGURE 5. MOMENTS OF THE DISTRIBUTION OF REAL WAGE CHANGES

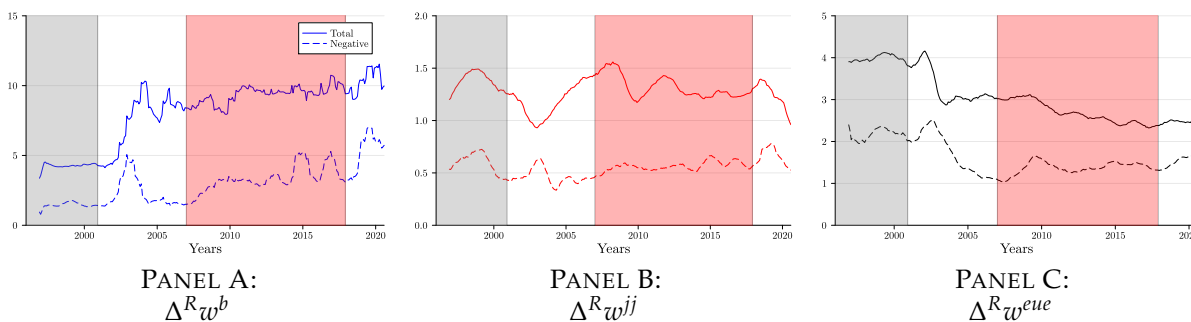


Notes: The figure shows the evolution of various moments of real wage changes from 1996 to 2021. Panels A to D display the median (P_{50}), the interquartile range ($P_{75} - P_{25}$), the Kelly skewness ($(P_{90} + P_{10} - 2P_{50}) / (P_{90} - P_{10})$), and the Crow-Siddiqui kurtosis ($(P_{97.5} - P_{2.5}) / (P_{75} - P_{25})$), respectively. The blue solid lines show the moments for real wage changes within jobs ($\Delta^R w^b$), the red dashed lines for job-to-job transitions without intervening unemployment spells, and the black dashed lines for job-to-job transitions with intervening unemployment spells. The shaded gray area highlights the low-inflation period (January 1996 - December 2000), and the shaded red area highlights the high-inflation period (January 2007 - December 2017). All variables are plotted on a $100 \times$ log scale.
Source: Data from SIPA.

also compute the fraction of real wage changes that are negative.

Three clear patterns emerge from the figure. First, the frequency of wage adjustments within jobs more than doubles, increasing from 4% in the low-inflation regime to 9% in the high-inflation regime, even without mechanisms of direct wage indexation.³ Under high inflation, approximately half of all adjustments result in *real* wage declines. Second, there is no change in the frequency of job-to-job transitions. Finally, wage changes after job separations become less frequent, and a higher share of them are associated with real wage decreases.

FIGURE 6. FREQUENCY OF WAGE CHANGES WITHIN AND ACROSS JOBS



Notes: The figure shows the frequency of wage changes within jobs (Panel A, denoted by $\Delta^R w^b$), the frequency of job-to-job transitions (Panel B, denoted by $\Delta^R w^{jj}$), and the frequency of job separations (Panel C, denoted by $\Delta^R w^{eue}$). All the plots also show the proportion of negative real wage changes associated with each frequency. The shaded gray area highlights the low-inflation period (January 1996 - December 2000), and the shaded red area highlights the high-inflation period (January 2007 - December 2017). Real wage changes are computed in the same month of a non-zero nominal change.

Source: Data from SIPA.

3 A Statistical Model of Wage Adjustment Across Inflation Regimes

The objective of this section is to develop a statistical Markov process for monthly labor income dynamics. The model extends the framework in [Guvenen et al. \(2021\)](#) along two key dimensions. First, leveraging the higher frequency of our data, we explicitly model monthly wage adjustments both within and across jobs. Second, motivated by the asymmetries observed in the distribution of wage changes, we incorporate state-contingent probabilities of wage adjustment. We next describe the law of motion governing labor income for an individual worker.

³Since the Ley de Convertibilidad (Law 23.928, 1991), Argentine law has prohibited formal indexation of contracts—including labor contracts—to inflation. This ban on automatic adjustments has remained in place even after the end of convertibility, though in practice frequent collective bargaining partly substitutes for formal indexation.

Description of Monthly Labor Income. The labor income process is characterized by seven components that jointly determine its law of motion. First, a worker's income depends on their employment status, denoted by $E \in \{h, u\}$, which indicates whether the worker is employed (h) or unemployed (u). Second, the process varies with the worker's age $a \in \{1, 2, \dots, A\}$ (measured in months) and the calendar month $m \in \{1, 2, \dots, 12\}$. Third, the worker is subject to two persistent idiosyncratic shocks: a permanent worker-specific component z , and a match-specific component ξ . In the absence of wage rigidities, wages would fully reflect these permanent components in each period. To capture the empirical patterns documented in the previous section, we model nominal rigidities by decomposing monthly wages into a contractual wage component w^C and a transitory deviation ϵ from it. Thus, the full state vector is given by $x = (E, z, \xi, \epsilon, w^C, a, m)$.

Each month, a worker may transition between employment and unemployment according to age- and productivity-dependent probabilities $p^{eu}(z, a)$ and $p^{ue}(z, a)$:

$$E' = \begin{cases} h, & \text{with probability } p^{ue}(z, a) \text{ if } E = u, \text{ or } 1 - p^{eu}(z, a) \text{ if } E = h, \\ u, & \text{with probability } 1 - p^{ue}(z, a) \text{ if } E = u, \text{ or } p^{eu}(z, a) \text{ if } E = h. \end{cases}$$

Conditional on the employment status E , the log real monthly earnings $y(x)$ for a worker in state x are given by:

$$y(x) = \mathbb{I}(E = u)(\log(B) + z) + \mathbb{I}(E = h)(\epsilon + w^C),$$

where $\mathbb{I}(\cdot)$ denotes the indicator function. Accordingly, an unemployed worker receives real income $B \exp(z)$, which captures government transfers and other income sources, while an employed worker earns $\exp(\epsilon + w^C)$. The transitory component ϵ is distributed as follows:

$$\epsilon \sim_{\text{i.i.d.}} \begin{cases} \mathcal{N}(\mu_\epsilon, \sigma_\epsilon), & \text{if } m \notin \{6, 12\} \text{ with probability } p_\epsilon, \\ 0, & \text{if } m \notin \{6, 12\} \text{ with probability } 1 - p_\epsilon, \\ \mathcal{N}(\mu_{\epsilon_{13}}, \sigma_{\epsilon_{13}}), & \text{if } m \in \{6, 12\} \end{cases} \quad (1)$$

This specification captures two stylized facts from Argentine labor data. First, it allows for month-specific distributions, reflecting the statutory 13th-month bonus, paid in two installments in June and December. Second, it accounts for the probability p_ϵ that workers experience transitory deviations from their contractual wage w^C . Both features are evident in Figure 2.

The evolution of a worker's contractual wage reflects three sources of variation. Whenever a worker either renegotiates their wage or transitions to a new job (from unemployment or another match), the

contract is reset based on the joint productivity term $z + \xi$. The probability of renegotiation, $p^b(\delta, m)$, is a function of the calendar month m and the deviation $\delta \equiv (z + \xi) - (w^C - \pi)$ between the target productivity-based wage and the current real contractual wage eroded by inflation. The probability of a job-to-job transition is denoted by $p^{jj}(z, a)$. The resulting law of motion for the real contractual wage is:

$$w^{C'}(x) = \begin{cases} z' + \xi', & \text{with probability } p^b(\delta, m) + (1 - p^b(\delta, m)) p^{jj}(z, a), \quad \text{if } E = h, E' = h, \\ w^C - \pi, & \text{with probability } (1 - p^b(\delta, m)) (1 - p^{jj}(z, a)), \quad \text{if } E = h, E' = h, \\ z' + \xi', & \text{if } E = u, E' = h, \end{cases} \quad (2)$$

We assume that the permanent worker-specific component z evolves according to:

$$\begin{aligned} z'(x) &= \theta_{1a}a + \theta_{2a}a^2 + \gamma_h \mathbb{I}(E = h) + \gamma_u \mathbb{I}(E = u) + z + v', \\ v' &\sim_{i.i.d.} \mathcal{N}(0, \sigma_v), \end{aligned} \quad (3)$$

where $\theta_{1a}a + \theta_{2a}a^2$ captures the average lifecycle profile, γ_h reflects human capital accumulation while employed and γ_u captures depreciation during unemployment. New labor market entrants ($a = 1$) draw their initial productivity from $z \sim \mathcal{N}(0, \sigma_0)$. The match-specific component ξ evolves as:

$$\xi'(x) \sim \begin{cases} \text{Sked}(\mu_{ue}, \sigma_{ue}, \tau_{ue}, \alpha_{ue}), & \text{if } E = u \text{ and } E' = h, \\ \text{Sked}(\mu_{jj}, \sigma_{jj}, \tau_{jj}, \alpha_{jj}), & \text{with probability } p^{jj}(z, a) \text{ if } E = h, \\ \xi, & \text{with probability } 1 - p^{jj}(z, a) \text{ if } E = h, \end{cases}$$

where $\text{Sked}(\cdot)$ denotes the skewed exponential power distribution with location μ , scale σ , skewness τ , and shape parameter α . The skewed exponential power distribution lets us match the excess kurtosis and asymmetric tails among switchers—see also [Carrillo-Tudela et al. \(2022\)](#) for empirical evidence of this process using occupational mobility in the US and [Hubmer \(2018\)](#) for the ability of these shocks to generate the US labor income process. Accordingly, the match component updates whenever the worker changes jobs, either through a job-to-job transition or following a spell of unemployment.

Following [Guvenen et al. \(2021\)](#), we parameterize all transition probabilities—job separation, job finding, job-to-job transitions, and wage bargaining—with a logistic function $\mathcal{L}(x) \equiv \exp(x)/(1 + \exp(x))$, where:

$$p^q(z, a) = \mathcal{L}(\theta_{0q} + \theta_{1q}z + \theta_{2q}a + \theta_{3q}za),$$

for $q \in \{eu, ue, jj\}$, and

$$p^b(\delta, m) = \mathcal{L} [\theta_{0b}\mathbb{I}(\delta > 0) (1 + \theta_{2b}\mathbb{I}(m = 6) + \theta_{3b}\mathbb{I}(m = 12)) + \theta_{1b}\mathbb{I}(\delta < 0) (1 + \theta_{2b}\mathbb{I}(m = 6) + \theta_{3b}\mathbb{I}(m = 12))].$$

This formulation enables flexible modeling of time-dependent patterns in wage bargaining. In particular, it allows the frequency of wage adjustments to vary in June and December and helps us, as shown below, to replicate the shifting nature of wage setting across inflation regimes.

Estimation and Identification. We estimate the statistical model using the same data restrictions as in Section 2. Each model period corresponds to a calendar month. The estimated parameters are summarized in Table 3.

To organize the empirical strategy, we distinguish between two types of data inputs. First, we use annualized earnings data to construct age-by-recent-income groupings, which are then used to condition moments calculated at the monthly frequency. Second, we use monthly earnings data to compute all moments.

We first construct groups of workers based on a measure of permanent income. Specifically, we compute each individual's total annual income in the previous year as a proxy for recent earnings. To isolate age effects, we regress this measure on a full set of age dummies for each year and define the residuals as recent earnings. We then assign workers in each year to age-income groups, using six age bins (e.g., 25-29, ..., 45-54) and deciles of the recent earnings distribution from the previous year. These groups are used to condition moments in the estimation procedure.

To discipline parameters affecting workers' initial condition and lifecycle component, we estimate the average lifecycle profile of real earnings. We pool all monthly observations and regress the log of real individual wages on a full set of age and year dummies. The estimated age coefficients identify the average lifecycle profile, which disciplines the parameters θ_{1a} and θ_{2a} in the law of motion for the permanent productivity component z . We then estimate the variance of log real earnings across individuals by age controlling for time effects. We match the empirical variance at age 25 to pin down the dispersion of initial productivity, σ_0 .

Next, we turn to wage and employment dynamics. Job-to-job transition and job-separation rates by income and age groups are used to discipline the parameters governing $p^{jj}(z, a)$ and $p^{eu}(z, a)$. The average unemployment rate of 11% and the observed job entry rates by income and age groups are used to identify the job-finding probability $p^{ue}(z, a)$.⁴ To align group-level flow rates with macroeconomic

⁴A job-to-job transition is defined as a direct move between employers without a gap; unemployment is defined as a temporary absence from the dataset. The entry rate is computed as the ratio of the number of workers in a given age-income group who enter the dataset in a given period to the total number of workers in that group.

targets, we rescale all transition rates across groups so that their average matches the corresponding aggregate rate observed in the data.

The evolution of the contractual wage is estimated using moments based on changes in $w_{i,t}^C$ obtained by applying the filter described in Section 2.1. We compute percentiles of the distribution of contractual wage changes within a job, conditional on a change having occurred. These moments, computed after winsorizing log wage changes at the 2nd and 98th percentiles, are informative about the dispersion of the permanent productivity shock σ_v and the parameters governing the asymmetry of wage bargaining outcomes. To discipline the frequency of wage renegotiation, we compute the monthly fraction of workers with no change in contractual wages, $\log w_{i,t}^C = \log w_{i,t-1}^C$, across the calendar year, and separately in June and December. These frequencies directly inform the specification of $p^b(\delta, m)$.

To identify the transitory component of wages, we restrict attention to observations where the contractual wage $w_{i,t}^C$ remains constant, and the employer is unchanged. Within this sample, we compute the mean and standard deviation of raw wages $\log w_{i,t} - \log w_{i,t-1}$ separately for June and December (when the 13th salary is paid) and for other selected months (April, May, September, and October).⁵ These differences help identify the parameters governing the transitory shock process. To discipline their incidence, we target the overall fraction of workers for whom the realized nominal wage $w_{i,t}$ remains unchanged from the previous month, which identifies the probability p_ϵ that a transitory wage adjustment occurs.

Finally, to capture the distribution of match-specific productivity shocks ζ , we compute wage changes around employment transitions. We calculate percentiles of winsorized contractual wage changes across job-to-job transitions, defined as $\log w_{i,t+1}^C - \log w_{i,t-2}^C$ conditional on a transition between consecutive months $t-1$ and t , and across unemployment-to-employment transitions, defined as $\log w_{i,t+1}^C - \log w_{i,t-j-1}^C$ for individuals who exited and re-entered employment between $t-j$ and t . These moments identify the parameters governing the distribution of ζ across different types of job flows.

Model fit. Figure 7 evaluates the model’s ability to replicate the distribution of non-zero contractual wage changes across different employment transitions. Panel A shows the distribution of wage changes within ongoing job spells, Panel B captures changes following job-to-job transitions without unemployment, and Panel C depicts changes following job-to-job transitions that involve at least one month of unemployment. In all three panels, the model closely approximates the dispersion and asymmetry of the empirical distributions. However, it struggles to match the sharp spike at zero and the prevalence of small changes

⁵These four months are chosen because they are unaffected by institutional or reporting distortions related to the 13th salary. In practice, the bonus can occasionally be paid early or late, introducing measurement error in adjacent months. By focusing on months without such confounding effects, we obtain cleaner estimates of transitory income shocks.

TABLE 3. ESTIMATED PARAMETERS FROM SMM

Parameter	Description	Values
Worker- and match-specific productivity		
(γ_e, γ_u)	Monthly drift of worker productivity	(0.002, 0.000)
(σ_0)	Std. dev. of initial worker productivity	0.485
(σ_v)	Std. dev. of worker productivity shocks	0.059
$(\theta_{1a}, \theta_{2a})$	Worker lifecycle profile	$(-1.000 \times 10^{-4}, 3.333 \times 10^{-9})$
$(\mu_{jj}, \sigma_{jj}, \tau_{jj}, \alpha_{jj})$	Distribution of jj match productivity	(0.000, 0.092, 1.776, 0.890)
$(\mu_{ue}, \sigma_{ue}, \tau_{ue}, \alpha_{ue})$	Distribution of ue match productivity	(0.000, 0.115, 0.800, 0.890)
Job transition probabilities		
$(\theta_{0ue}, \theta_{1ue}, \theta_{2ue}, \theta_{3ue})$	Job-finding probability (logistic coefficients)	(-0.500, -0.787, -0.001, -0.000)
$(\theta_{0eu}, \theta_{1eu}, \theta_{2eu}, \theta_{3eu})$	Separation probability (logistic coefficients)	(-2.969, -0.803, -0.001, -0.000)
$(\theta_{0jj}, \theta_{1jj}, \theta_{2jj}, \theta_{3jj})$	Job-to-job transition probability (logistic coefficients)	$(-4.130, -0.800, -0.001, -3.125 \times 10^{-4})$
Transitory shocks		
$(\mu_{\epsilon_{13}}, \sigma_{\epsilon_{13}})$	Mean and std. dev. of 13-th wage bonus	(0.411, 0.140)
$(p_{\epsilon}, \mu_{\epsilon}, \sigma_{\epsilon})$	Probability, mean, and std. dev. of transitory wage shock	(0.680, 0.000, 0.126)
Wage changes within jobs		
$(\theta_{0b}, \theta_{1b}, \theta_{2b}, \theta_{3b})$	Wage adjustment rate (logistic coefficients) — Low inflation	(-0.350, -0.300, -4.100, -2.900)
$(\theta_{0b}, \theta_{1b}, \theta_{2b}, \theta_{3b})$	Wage adjustment rate (logistic coefficients) — High inflation	(-0.670, -0.710, -6.400, -2.400)

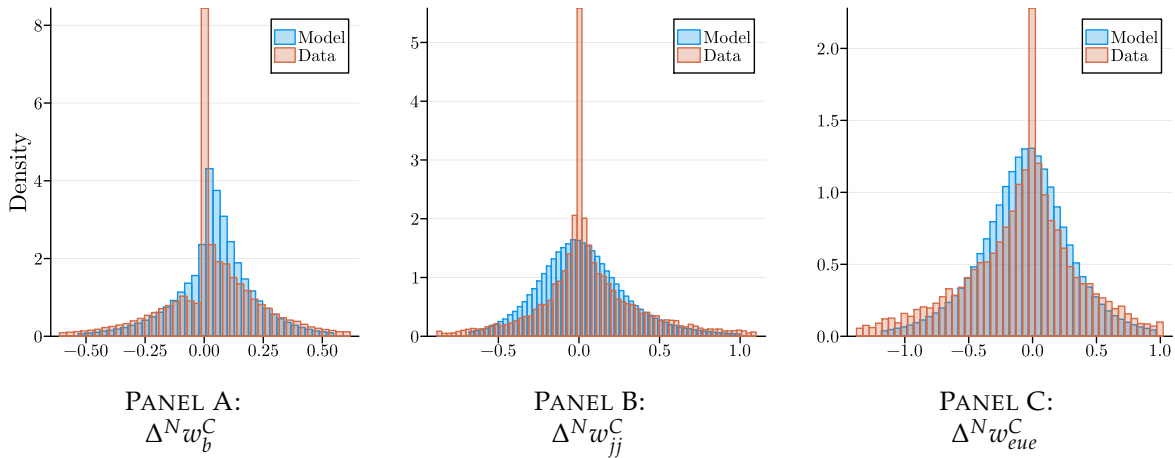
Notes: The table presents the estimated values assigned to the real wage process. We set the average annual inflation rate in the low-inflation regime to -0.12% .

observed in the data, especially in transitions across jobs.

Figure 8 compares the empirical and simulated job-to-job transition rates by age and income deciles. Panel A presents the rates observed in the data, while Panel B shows the corresponding model-implied values. The model matches the declining pattern of transition rates across the earnings distribution and reasonably captures the age gradient, although it slightly underpredicts transitions among the youngest and lowest-income groups. Similarly, Figure 9 examines employment-to-unemployment transition rates by age and income groups. Again, the model reproduces the steep decline in separation probabilities with income and the relative flatness across age within each earnings decile. Figure 10 shows that the model is able to replicate well the unemployment-to-employment entry rates by age and income groups.

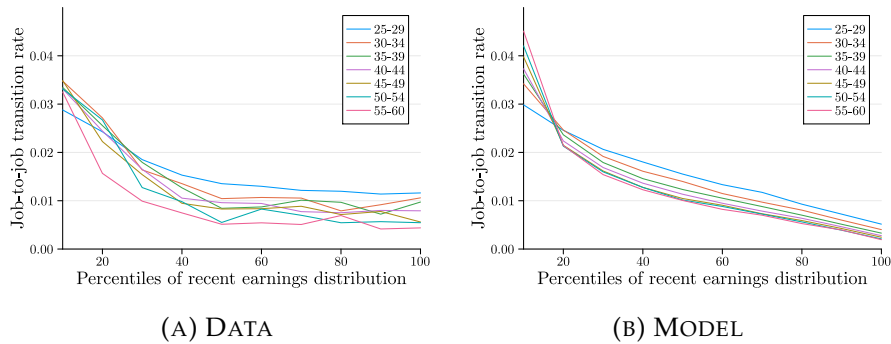
Finally, Table 4 presents a summary of the remaining targeted moments in both the data and the simulated model. The model matches these moments quite closely.

FIGURE 7. NON-ZERO CONTRACTUAL WAGE CHANGES WITHIN AND ACROSS JOBS



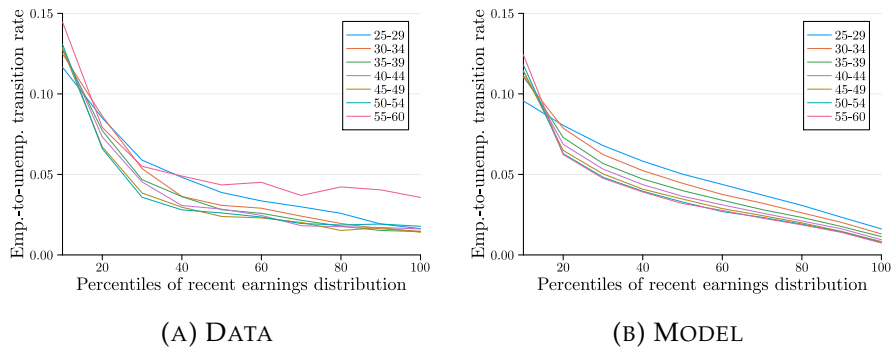
Notes: The figure shows the densities of non-zero nominal contractual wage changes within job spells (Panel A, denoted by $\Delta^N w_b^C$), following job-to-job transitions without intervening spells of unemployment (Panel B, denoted by $\Delta^N w_{jj}^C$), and following job-to-job transitions with at least one month of unemployment (Panel C, denoted by $\Delta^N w_{eue}^C$) at low inflation. The blue bars show densities for the data and the red bars represent the model. For these plots, we truncate each distribution from the data at the 2nd and 98th percentiles. Source: Data from SIPA and authors' calculations.

FIGURE 8. JOB-TO-JOB TRANSITION RATE



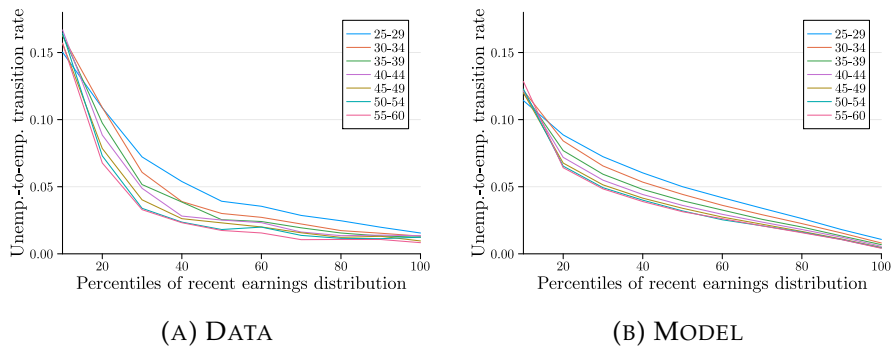
Notes: The figure shows the job-to-job transition rate by age and income groups. The data moments are computed from 1996 to 2020. Panel A shows the empirical job-to-job transition rate, while Panel B shows the simulated job-to-job transition rate. Source: Data from SIPA.

FIGURE 9. EMPLOYMENT-TO-UNEMPLOYMENT TRANSITION RATE



Notes: The figure shows the employment-to-unemployment transition rate by age and income groups. The data moments are computed from 1996 to 2020. Panel A shows the empirical employment-to-unemployment transition rate, while Panel B shows the simulated employment-to-unemployment transition rate. Source: Data from SIPA.

FIGURE 10. UNEMPLOYMENT-TO-EMPLOYMENT ENTRY RATE



Notes: The figure shows the transition rate by age and income groups. The data moments are computed from 1996 to 2020. Panel A shows the empirical entry rate, while Panel B shows the simulated entry rate. Source: Data from SIPA.

TABLE 4. GOODNESS OF FIT: MODEL VS. DATA

Description	Data	Model
Aggregate unemployment rate	0.112	0.111
Frequency of constant raw wages within a job	0.064	0.066
Frequency of constant contractual wages within a job	0.954	0.958
Frequency of constant contractual wages within a job in June	0.929	0.918
Frequency of constant contractual wages within a job in December	0.915	0.905
Avg. log raw earnings growth in June/December	0.411	0.411
Standard deviation of log raw earnings growth in June/December	0.172	0.174
Avg. log raw earnings growth in other months	0.006	0.000
Standard deviation of log raw earnings growth in other months	0.144	0.147

Notes: The table compares selected targeted moments in the data and the model simulated under the low-inflation regime. The model is estimated using the method of simulated moments (SMM). Raw wages refer to total monthly labor income, and contractual wages refer to the permanent component of realized wages. Log earnings growth is computed as the change in log real wages between consecutive months. *Source:* Data from SIPA and authors' calculations.

4 The Consumption-Savings Problem and the Cost of Inflation

This section integrates our estimated labor income risk into a consumption-savings decision problem to quantify the welfare cost of inflation.

Environment. There is a continuum of workers who live in a small open economy. Workers are heterogeneous in their asset holdings n and monthly labor income $\exp(y)$. Each worker chooses consumption and savings to maximize expected lifetime utility. Preferences are characterized by a constant relative risk aversion (CRRA) utility function with risk aversion parameter φ and discount factor β :

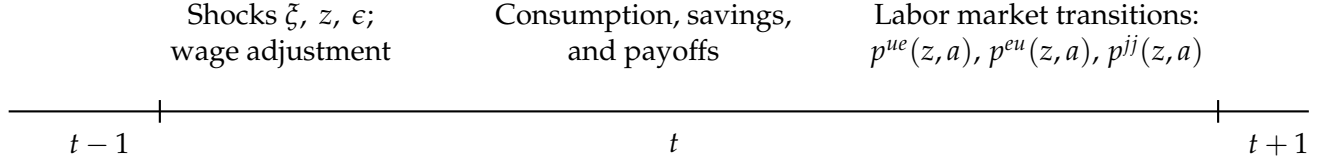
$$\mathbb{E} \left[\sum_{a=1}^A \beta^a \frac{c_a^{1-\varphi}}{1-\varphi} \right].$$

Workers can save in a risk-free asset with return r , subject to a no-borrowing constraint $n' \geq 0$.

Timing within the Period. The timing within each period unfolds as follows. At the beginning of the period, idiosyncratic shocks z , ϵ , and ζ are realized. Conditional on these shocks, the wage may be adjusted. The worker then chooses consumption and savings. Finally, labor market transitions take place:

unemployed workers may find a job, while employed workers may either separate into unemployment or transition to another job. Figure 11 summarizes the timing within the period.

FIGURE 11. TIMING WITHIN A PERIOD



Recursive Formulation. Let $U_a(n, z, m)$ denote the lifetime expected utility of an *unemployed* worker with asset holdings n , productivity z at age a and calendar month m . Similarly, let $H_a(n, \xi, z, \epsilon, w^C, m)$ denote the lifetime expected utility of an *employed* worker with asset holdings n . Workers live for A periods, thus the terminal conditions are:

$$U_{A+1}(n, z, m) = H_{A+1}(n, \xi, z, \epsilon, w^C, m) = 0.$$

The recursive problem of an unemployed worker for all $a \leq A$ is given by:

$$U_a(n, z, m) = \max_{c_u, n'_u} \left\{ \frac{c_u^{1-\varphi}}{1-\varphi} + \beta \mathbb{E}_{\xi'_{ue}, z'_u, \epsilon'_m} \left[p^{ue}(z, a) H_{a+1}(n'_u, \xi'_{ue}, z'_u, \epsilon'_m, \xi'_{ue} + z'_u, m') \right. \right. \\ \left. \left. + (1 - p^{ue}(z, a)) U_{a+1}(n'_u, z'_u, m') \mid z, m \right] \right\} \quad (4)$$

subject to the budget constraint

$$\frac{n'_u}{1+r} + c_u = n_u + Be^z \quad \text{and} \quad n'_u \geq 0. \quad (5)$$

Unemployed workers receive home production income Be^z , choose consumption c and next-period savings n' , and face a no-borrowing constraint $n' \geq 0$. With probability $p^{ue}(z, a)$, they find a job and draw a new match-specific component $\xi'_{ue} \sim \text{Sked}(\mu_{ue}, \sigma_{ue}, \tau_{ue}, \alpha_{ue})$. The unemployed worker's productivity z'_u evolves according to (3), and the starting contractual wage is $\xi'_{ue} + z'_u$. The transitory shock ϵ'_m follows (1), with the calendar month updating deterministically.

The recursive problem of an employed worker for all $a \leq A$ is given by:

$$\begin{aligned}
H_a(n, \xi, z, \epsilon, w^C, m) = \max_{c_h, n'_h \geq 0} & \left\{ \frac{c_h^{1-\varphi}}{1-\varphi} + \beta \mathbb{E}_{\xi'_{jj}, z'_h, \epsilon'_m} \left[p^{eu}(z, a) U_{a+1}(n'_h, z'_h, m') \right. \right. \\
& + (1 - p^{eu}(z, a)) p^{jj}(z, a) H_{a+1}(n'_h, \xi'_{jj}, z'_h, \epsilon'_m, \xi'_{jj} + z'_h, m') \\
& + (1 - p^{eu}(z, a)) \left(1 - p^{jj}(z, a) \right) \left(1 - p^b(\delta', m) \right) H_{a+1}(n'_h, \xi, z'_h, \epsilon'_m, w^C - \pi, m') \\
& \left. \left. + (1 - p^{eu}(z, a)) \left(1 - p^{jj}(z, a) \right) p^b(\delta', m) H_{a+1}(n'_h, \xi, z'_h, \epsilon'_m, \xi + z'_h, m') \mid z, m \right] \right\} (6)
\end{aligned}$$

with $\delta' = \xi + z'_h - (w^C - \pi)$ and subject to a similar budget constraint (5) but with labor income replacing home production Be^z . Employed workers earn labor income $e^{\epsilon+w^C}$, where w^C is the real contractual wage and ϵ is a transitory shock. In the next period: (i) with probability $p^{eu}(z, a)$, the worker becomes unemployed; (ii) otherwise, with probability $p^{jj}(z, a)$, the worker transitions to a new job with match-specific component $\xi'_{jj} \sim \text{Sked}(\mu_{jj}, \sigma_{jj}, \tau_{jj}, \alpha_{jj})$, and (iii) if the worker stays in the same job, they renegotiate the wage with probability $p^b(\delta', m)$, resetting it to $\xi + z'_h$ (with the remaining probability, the real wage erodes at rate π , becoming $w^C - \pi$).

Parametrization. A period in the model corresponds to one month. The model features two sets of parameters: those related to the stochastic process of labor income and those governing preferences and the interest rate. The parameters of the income process are described in Table 3. Home production is set to $B = 0.2$, consistent with the average income loss following job displacement observed in household survey data from Argentina. The coefficient of relative risk aversion is set to $\varphi = 2$.

Parametrizing the discount factor β and the real return on assets r requires special attention. Two observations guide our calibration strategy: (i) welfare calculations require a realistic treatment of discounting and asset accumulation in order to capture precautionary savings; and (ii) although the model abstracts from asset heterogeneity (such as liquid versus illiquid assets), we interpret assets as liquid, since they can be adjusted at a monthly frequency without frictions.

Given these considerations, we follow [Kaplan and Violante \(2014\)](#) and set the annualized real return on liquid assets to -1.5% , consistent with U.S. estimates during a period of low inflation. We interpret -1.5% as an upper bound on the rate of return of liquid assets, reflecting the deep financial markets and macroeconomic stability in the U.S. relative to Argentina. Importantly, given that the interest rate of liquid assets is negative, buffer-stock savings for anticipated shocks are costly.

In our baseline calibration, we keep the same rate of return in the high-inflation scenario, implying that

financial assets are fully indexed to inflation. This assumption allows us to isolate the new mechanism of interest—real income dynamics—while avoiding confounding effects from asset returns. Nevertheless, we also report robustness analyses using a lower annual return of -10% .

We set the annualized discount factor to $\beta = 0.9$, which lies at the lower end of values used in the literature. Under this parametrization, the model predicts a median liquid-asset-to-income ratio of 5.2—well above its empirical counterpart—and a mean of 6.6. For comparison, [Kaplan and Violante \(2014\)](#) report a median ratio of 0.5 and mean of 7, while [Ferrante and Gornemann \(2022\)](#) document that approximately 80% of households in Uruguay, a comparable neighboring country, hold zero or negative liquid wealth.

To summarize, our choice of return and discount factor is conservative and likely understates the welfare costs of inflation, providing a lower bound for our results. In our robustness checks, we explore an alternative model with hand-to-mouth workers which can be considered as an upper bound.

In what follows, we conduct a baseline exercise complemented with three robustness checks. The benchmark approach modifies the stochastic process of labor income in two dimensions to eliminate differences in average real wages across inflation regimes. First, we introduce a positive reset wage that offsets expected future inflation and ensures that the average level of real wages remains the same across regimes. In particular, we modify the stochastic process in (2):

$$w^{C'}(x) = \begin{cases} w^* + z' + \zeta', & \text{with probability } p^b(\delta, m) + (1 - p^b(\delta, m)) p^{jj}(z, a), & \text{if } E = h, E' = h, \\ w^C - \pi, & \text{with probability } (1 - p^b(\delta, m)) (1 - p^{jj}(z, a)), & \text{if } E = h, E' = h, \\ w^* + z' + \zeta', & \text{if } E = u, E' = h, \end{cases}$$

Second, we adjust the argument of the wage-adjustment probability, setting $\delta = (w^* + z + \zeta) - (w^C - \pi)$. With these two modifications, the reset wage w^* shifts the average level of real wages without altering their law of motion.

We calibrate the reset wage w^* so that average real wages are comparable across regimes. There is, however, a caveat. In our model—as in all Bewley-Aiyagari models— $\beta(1 + r) < 1$, so raising current income at the expense of future income increases welfare. In the extreme case of risk-neutral, hand-to-mouth households, this reallocation increases welfare purely due to high discounting. To address this, we set $w^* = 0$ in the low-inflation regime and choose $w^* = 0.1$ in the high-inflation regime to ensure that the *present discounted value* of real wages remains the same across regimes when using the household discount factor β ; i.e., $\mathbb{E} \left[\sum_{a=1}^A \beta^a w_a \right]$ is identical across regimes. Under this specification, risk-neutral and hand-to-mouth consumers are indifferent between the two inflation regimes, so any remaining welfare

difference is driven purely by the volatility of real wages rather than their average level.

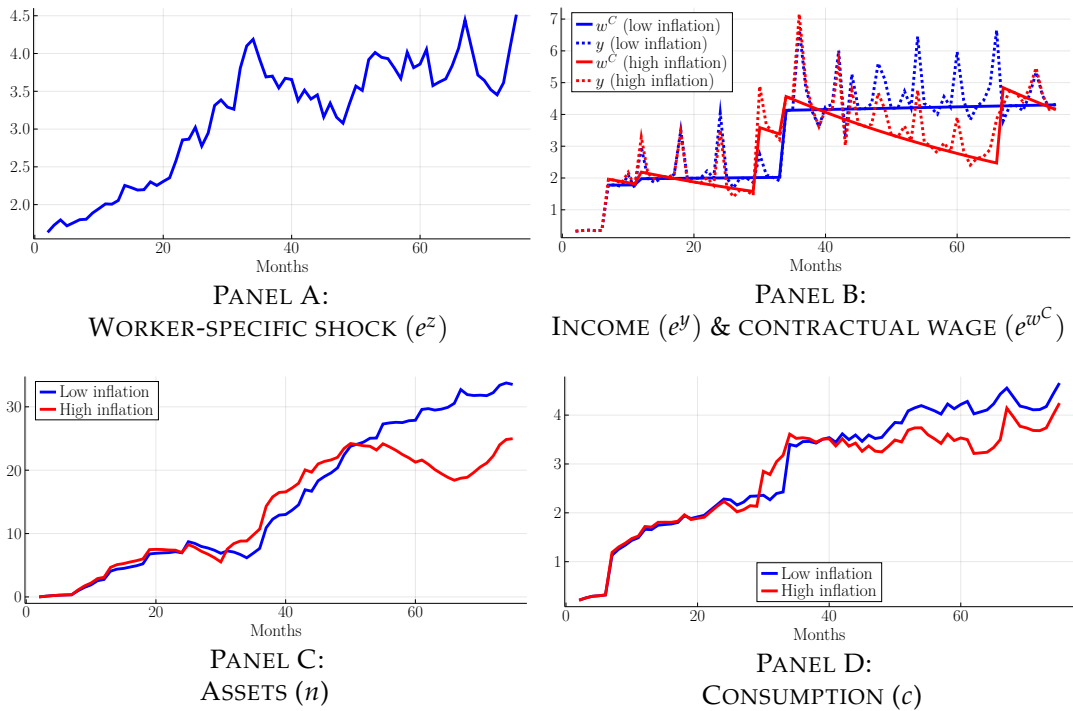
Economic Mechanisms. We now analyze optimal consumption-saving decisions in response to labor income shocks and the effect of inflation. Figure 12 illustrates the model's predictions for the same sequence of shocks under low inflation (in blue) and high inflation (in red) during the first six years of a worker's career. Panels A to D display the worker-specific productivity shock, monthly income and contractual wage, asset holdings, and consumption, respectively. In this simulation, match-specific shocks are held constant.

Consider first the low-inflation environment. From months 1 to 7, the worker is unemployed and asset holdings remain close to the borrowing limit. In month 7, the worker finds a job. Given the low probability of separation, the increase in income results in a highly persistent income gain. Consequently, consumption jumps upward, with smaller additional increases observed in June and December. Around month 25, the worker experiences a persistent increase in productivity. Because wage adjustments are infrequent, the current wage remains low, leading to an anticipated rise in future income. To smooth consumption, the worker reduces savings and asset holdings during these

In the high-inflation scenario, unemployment income remains unchanged, and the positive reset wage ensures that the present discounted value of real wages is comparable across regimes. However, the dynamics of real wages within employment spells differ markedly. Between wage adjustments, real wages erode faster due to higher inflation, generating larger and more frequent drops in real income. When renegotiation occurs, the reset wage partially compensates for this erosion, producing a pronounced sawtooth pattern in contractual wages. Because wage adjustments are more frequent under high inflation, contractual wages track productivity shocks more closely. Despite similar average income levels, the greater volatility of real wages induces larger swings in consumption: the worker draws down savings during periods of unexpectedly prolonged wage erosion and rebuilds them upon renegotiation. This additional consumption volatility—driven entirely by differences in the time path of real wages rather than their average level—is the key channel through which inflation reduces welfare.

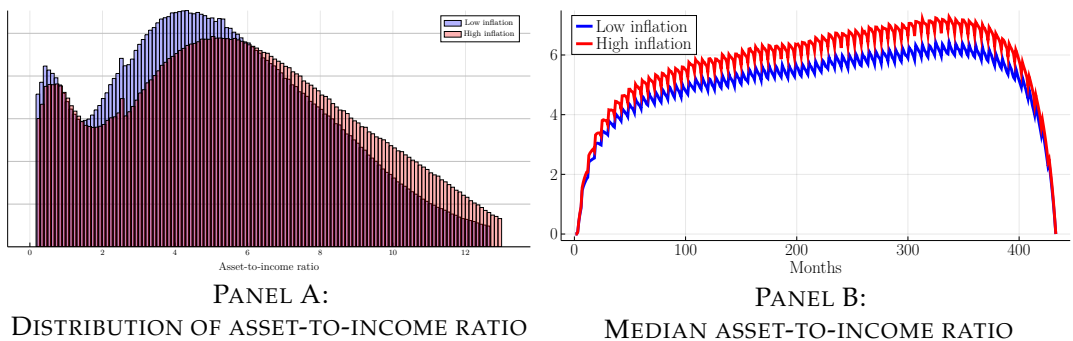
Figure 13, Panel A, shows the distribution of liquid assets relative to income in the model—abstracting from transitory shocks to ease exposition—for both the low- and high-inflation regimes. The model predicts a higher asset-to-income ratio under high inflation, which is consistent with the larger negative drift in real labor income caused by wage erosion. Finally, the model exhibits an inverse U-shaped life-cycle profile for median asset-to-income ratios, as shown in Figure 13, Panel B.

FIGURE 12. OPTIMAL CONSUMPTION: LOW VS. HIGH INFLATION



Notes: The figure illustrates the sample path for a worker with a given sequence of shocks under low inflation (blue) and high inflation (red) over the first six years of their career. The worker is born in January, and the match-specific shock is held constant by construction. The figure shows the worker-specific productivity shock, monthly income and contractual wage, asset holdings, and consumption.
 Source: Authors' calculations.

FIGURE 13. MOMENTS OF THE ASSET-TO-INCOME RATIO DISTRIBUTION



Notes: The figure shows the distribution of the asset-to-income ratio (Panel A) and the median asset-to-income ratio over the life cycle of a worker (Panel B). For the income measure, we only consider its permanent component: Be^z if unemployed and e^{w^C} if employed.
 Source: Authors' calculations.

Welfare Effects. Having described the response of optimal consumption and savings decisions to higher inflation, we now ask: upon entering the labor market, what compensation would make a worker indifferent between living in a high-inflation economy (22%) and one with zero inflation? To answer this question, let $U_1^{\pi=0}(0, z, 1)$ and $U_1^{\pi=22}(0, z, 1)$ denote the lifetime utility of a newly born unemployed worker of type z , entering the labor market with zero assets under 0% and 22% trend inflation, respectively. By definition and exploiting homotheticity of preferences, the consumption equivalent variation $\mathbf{CV}(z)$ (in percentage terms) satisfies:

$$U_1^{\pi=0}(0, z, 1) = \left(1 + \frac{\mathbf{CV}(z)}{100}\right)^{1-\varphi} U_1^{\pi=22}(0, z, 1),$$

or equivalently,

$$\mathbf{CV}(z) = \left[\left(\frac{U_1^{\pi=0}(0, z, 1)}{U_1^{\pi=22}(0, z, 1)} \right)^{\frac{1}{1-\varphi}} - 1 \right] \times 100.$$

Here, $\mathbf{CV}(z)$ denotes the constant percentage increase in monthly consumption, sustained over the entire working life, that would make a worker in a high-inflation economy indifferent to living in a low-inflation economy. The aggregate version of this statistic is given by:

$$\mathbf{CV} = \int_{-\infty}^{\infty} \mathbf{CV}(z) f(z, \sigma_0) dz,$$

where $f(z, \sigma_0)$ denotes the normal density with mean zero and standard deviation σ_0 .

Table 5 reports the consumption-equivalent variation both in the aggregate and across quintiles of the worker initial productivity distribution. At the aggregate level, a worker facing 22% inflation instead of 0% inflation would require compensation equal to 1.02% of monthly consumption, over the entire working life, to be indifferent.

Welfare costs are smaller for workers in the lower productivity quintiles, ranging from -0.12% in the lowest quintile to 2.12% in the highest quintile. Two mechanisms help explain this pattern. First, lower-income workers experience greater labor market mobility, increasing their chances of switching jobs and resetting their wages, thereby limiting the erosion of real wages during high-inflation periods. Second, they face higher unemployment risk and rely more on home production income, which is fixed in real terms and therefore protected from inflation. Together, these forces result in lower welfare losses at the bottom of the productivity distribution. Moreover, because preferences are homothetic, saving behavior does not vary systematically with permanent income, which further dampens the role of asset heterogeneity across quintiles.

TABLE 5. WELFARE COST OF INFLATION

	Baseline ($w^* = 0.1$)	Robustness		
		Hand-to-mouth	Lower real rate ($r = -10\%$)	No discounted income
CV	1.02	2.04	2.92	7.68
Quintiles				
CV(z)-1st	-0.12	0.82	1.73	6.06
CV(z)-2nd	0.55	1.52	2.43	7.01
CV(z)-3rd	1.04	2.05	2.94	7.71
CV(z)-4th	1.52	2.58	3.44	8.40
CV(z)-5th	2.12	3.25	4.05	9.21

Notes: The table reports the aggregate consumption-equivalent variation (in percentage terms) for a worker living in a 22% inflation economy relative to a 0% inflation economy. The first row shows the aggregate value, while the following rows present results across quintiles of the worker productivity distribution. The last three columns report robustness checks, varying the set of available savings instruments, the real interest rate, and the assumption regarding how average real labor income changes across inflation regimes.

Source: Authors' calculations.

Robustness. We now assess the robustness of our main findings through a set of alternative parametrizations and exercises. In the first exercise, we assume that households are hand-to-mouth, meaning consumption equals income in every period. The second column in Table 5 reports the resulting consumption-equivalent variation. As expected, both aggregate and distributional welfare costs of inflation are larger, since households cannot smooth consumption over time. Nonetheless, the magnitudes remain comparable to our baseline both in the aggregate and across the distribution.

In the second exercise, we consider a lower real interest rate in the high-inflation regime. World Bank data indicate that the average nominal deposit rate during this period was 16%. Given prevailing inflation, this implies a real return of about -7% , providing an upper bound for the real return on liquid assets. At the other extreme, if households hold only money, the real return is -22% , a natural lower bound. We therefore assume a real interest rate of -10% for the high-inflation period, closer to that upper bound. The results of this exercise are reported in the third column of Table 5: The aggregate consumption-equivalent welfare cost is higher than both the baseline case and the hand-to-mouth specification. Also, a more negative real interest rate increases the welfare cost of inflation for higher-productivity workers, who hold more liquid assets.

In the last exercise, we set $w^* = 0$ across both inflation regimes. Thus, the average real wage in the low-inflation period is greater than its high-inflation counterpart. The last column of Table 5 shows that the consumption-equivalent variation is higher than in the baseline and the remaining robustness checks:

a worker would still be willing to forgo 7.68% of monthly consumption to live in a low-inflation economy. Overall, these exercises demonstrate that our main result is robust to alternative parametrizations and modeling assumptions.

5 Conclusion

This paper quantifies a novel welfare cost of inflation that arises from the erosion of real wages in the presence of incomplete markets and nominal wage rigidity. Drawing on high-frequency administrative data from Argentina, we document that real wage dynamics differ significantly across inflation regimes. To quantify the implications of these different wage dynamics for household welfare, we estimate a statistical model of wage adjustment and embed it within a Bewley-Aiyagari framework. The model successfully replicates key empirical patterns and implies a consumption-equivalent welfare loss of 1.02% when moving from a 0% to a 22% inflation environment.

Our results suggest that even moderate levels of trend inflation can generate substantial welfare losses once nominal wage rigidity and market incompleteness are taken into account. More broadly, the findings underscore the need to incorporate labor market frictions and heterogeneous income dynamics into evaluations of optimal inflation policy. While our analysis isolates the labor income channel, other mechanisms likely amplify these effects for lower-income households. First, the prices of goods in these households' consumption baskets tend to be more volatile ([Cravino and Levchenko, 2017](#)). Second, they typically have a higher marginal propensity to consume and spend a larger share of their income on necessities, leaving them with smaller buffers ([Kaplan and Violante, 2014](#)). Third, the incomplete indexing of social transfers and unemployment benefits can lead to significant real income erosion. Conversely, evidence from Argentina suggests that the frequency of wage adjustments increases toward the bottom of the income distribution ([Blanco *et al.*, 2022](#)), which may partially mitigate these welfare costs for the poor relative to high-income workers. Finally, as high inflation is typically accompanied by higher inflation volatility, a fruitful research avenue is to examine how such volatility interacts with asset returns and market incompleteness to further impact household welfare.

References

- AFROUZI, H., BLANCO, A., DRENİK, A. and HURST, E. (2026). A Theory of How Workers Keep up with Inflation. *The Quarterly Journal of Economics*, pp. 1–60.
- ALLAIS, O., ALGAN, Y., CHALLE, E. and RAGOT, X. (2020). The Welfare Cost of Inflation Risk under Imperfect Insurance. *Annals of Economics and Statistics*, (138), 1–20.
- BAUMOL, W. J. (1952). The Transactions Demand for Cash: An Inventory Theoretic Approach. *The Quarterly Journal of Economics*, **66** (4), 545–556.
- BLANCO, A. (2020). Optimal Inflation Target in an Economy with Menu Costs and an Occasionally Binding Zero Lower Bound. *American Economic Journal: Macroeconomics*.
- , DÍAZ DE ASTARLOA, B., DRENİK, A., MOSER, C. and TRUPKIN, D. R. (2022). The Evolution of the Earnings Distribution in a Volatile Economy: Evidence from Argentina. *Quantitative Economics*, **13**, 1361–1403.
- , DRENİK, A., MOSER, C. and ZARATIEGUI, E. (2024). *A Theory of Labor Markets with Inefficient Turnover*. Working Paper 32409, National Bureau of Economic Research.
- , — and ZARATIEGUI, E. (2025). Nominal Devaluations, Inflation and Inequality. *American Economic Journal: Macroeconomics*, **17** (3), 270–310.
- CARRILLO-TUDELA, C., VISSCHERS, L. and WICZER, D. (2022). Cyclical Earnings, Career and Employment Transitions.
- CARROLL, C. D. (2006). The Method of Endogenous Gridpoints for Solving Dynamic Stochastic Optimization Problems. *Economics Letters*, **91** (3), 312–320.
- CRAVINO, J. and LEVCHENKO, A. (2017). The Distributional Consequences of Large Devaluations. *American Economic Review*, **107** (11), 3477–3509.
- EROSA, A. and VENTURA, G. (2002). On Inflation as a Regressive Consumption Tax. *Journal of Monetary Economics*, **49** (4), 761–795.
- FELDSTEIN, M. (1976). Inflation, Income Taxes, and the Rate of Interest: A Theoretical Analysis. *American Economic Review*, **66** (5), 809–820.
- FERRANTE, F. and GORNEMANN, N. (2022). Devaluations, Deposit Dollarization, and Household Heterogeneity. *International Finance Discussion Paper*, (1336).
- FRIEDMAN, M. (1969). *The Optimum Quantity of Money and Other Essays*. Chicago: Aldine Publishing Company.
- GANONG, P., NOEL, P., PAVAN, A., VAVRA, J. and WEBER, M. (2024). Earnings Instability. *Working paper*.
- GUVENEN, F., KARAHAN, F., OZKAN, S. and SONG, J. (2021). What Do Data on Millions of US Workers Reveal about Lifecycle Earnings Dynamics? *Econometrica*, **89** (5), 2303–2339.
- HUBMER, J. (2018). The Job Ladder and its Implications for Earnings Risk. *Review of Economic Dynamics*, **29**, 172–194.
- İMROHOROĞLU, A. (1992). The Welfare Cost of Inflation under Imperfect Insurance. *Journal of Economic Dynamics and Control*, **16** (1), 79–91.
- KAPLAN, G. and VIOLANTE, G. L. (2014). A Model of the Consumption Response to Fiscal Stimulus Payments. *Econometrica*, **82** (4), 1199–1239.
- STEVENS, L. (2020). Coarse Pricing Policies. *The Review of Economic Studies*, **87** (1), 420–453.

**Wage Erosion with Incomplete Markets:
A Quantitative Analysis of the Costs of Inflation**

Online Appendix—Not for Publication

Contents of the Online Appendix

A	Data: Additional Results	A1
B	Normalized Value Functions and Consumption Equivalent	B1
C	Computational notes	C1

A Data: Additional Results

Table A1 describes the publicly available SIPA dataset.

TABLE A1. VARIABLES IN SIPA PUBLIC AVAILABLE DATA

Variable	Years in data	Short description
Worker's variables		
Worker identification number	1996m1-2021m12	Social Security Number (CUIL)
Gender	1996m1-2021m12	
Age	1996m1-2021m12	
Firm's variables		
Job identifier	1996m1-2021m12	
State	1996m1-2021m12	State in which the firm is registered
Industry	1996m1-2021m12	4-digit CIU
Labor income components		
Total labor income	1996m1-2021m12	Nominal in pesos (per month)

Notes: The table describes the variables in SIPA, along with the years of coverage in the sample.

TABLE A2. REAL WAGE CHANGES SUMMARY STATISTICS

	Monthly (nonzero)		Monthly		Annual	
	Low	High	Low	High	Low	High
Percentiles						
P2.5	-52.57	-30.10	-1.24	-1.93	-37.45	-26.07
P25	-9.05	1.86	0.01	-1.86	0.20	-5.78
P50	0.32	12.11	0.01	-1.86	0.20	3.46
P75	11.09	23.24	0.01	-0.76	2.17	13.12
P97.5	62.09	65.05	4.10	20.18	48.07	52.61

Notes: The table reports summary statistics for distribution of real wage adjustments during low- and high-inflation periods. Real wage changes $\Delta^R w$ are calculated as nominal wage growth net of contemporaneous inflation. The first two columns comprise the entire distribution, excluding nil adjustments. The remaining columns include zero changes. Annual wage changes are computed on a year-to-year basis. All statistics are computed from the non-truncated distributions.

B Normalized Value Functions and Consumption Equivalent

In our model, consumption and savings are proportional to worker-specific productivity. This proportionality becomes exact if the transition probabilities $p^{ue}(z, a)$, $p^{eu}(z, a)$, and $p^{jj}(z, a)$ are independent of z . We leverage this feature by rescaling the value and policy functions by z . Additionally, we use cash-in-hand as a state variable and the timing convention that $a = 1$ when $m = 1$. These assumptions altogether simplify the numerical solution to the consumption-savings problem. We summarize this result with the following proposition.

Proposition B.1. *Let $U_a(n, z, m)$ and $H_a(n, \zeta, z, \epsilon, w^C, m)$ satisfy the recursions (4) and (6). Assume that all workers are born in January, i.e., $a = 1$ when $m = 1$. Then*

$$U_a(n, z, m) = e^{(1-\varphi)z} \tilde{U}_a \left(\frac{n + Be^z}{e^z}, z \right)$$

$$H_a(n, \zeta, z, \epsilon, w^C, m) = e^{(1-\varphi)z} \tilde{H}_a \left(\frac{n + e^{\epsilon+w^C}}{e^z}, \zeta, z, w^C - z \right)$$

where $\tilde{U}_a(\tilde{\omega}, z)$ and $\tilde{H}_a(\tilde{\omega}, \zeta, \tilde{w}^C, z)$ satisfy for all $a \leq A$ the recursions

$$\tilde{U}_a(\tilde{\omega}, z) = \max_{\tilde{c}_u, \tilde{n}'_u \geq 0} \left\{ \frac{\tilde{c}_u^{1-\varphi}}{1-\varphi} + \beta \mathbb{E}_{\xi'_{ue}, z'_u, \epsilon'_a} \left[e^{(1-\varphi)(z'_u - z)} \left[p^{ue}(z, a) \tilde{H}_{a+1} \left(\tilde{n}'_u e^{z-z'_u} + e^{\epsilon'_a + \xi'}, \xi'_{ue}, z'_u, \xi'_{ue} \right) \right. \right. \right. \\ \left. \left. \left. + (1 - p^{ue}(z, a)) \tilde{U}_{a+1} \left(\tilde{n}'_u e^{z-z'_u} + B, z'_u \right) \right] \middle| z \right] \right\}$$

$$\frac{\tilde{n}'_u}{1+r} + \tilde{c}_u = \tilde{\omega}$$

$$\tilde{H}_a(\tilde{\omega}, \zeta, z, \tilde{w}^C) = \max_{\tilde{c}_h, \tilde{n}'_h \geq 0} \left\{ \frac{\tilde{c}_h^{1-\varphi}}{1-\varphi} + \beta \mathbb{E}_{\xi'_{jj}, z'_h, \epsilon'_a} \left[e^{(1-\varphi)(z'_h - z)} \left[p^{eu}(z, a) \tilde{U}_{a+1} \left(\tilde{n}'_h e^{z-z'_h} + B, z'_h \right) \right. \right. \right. \\ \left. \left. \left. + (1 - p^{eu}(z, a)) p^{jj}(z, a) \tilde{H}_{a+1} \left(\tilde{n}'_h e^{z-z'_h} + e^{\epsilon'_a + \xi'_{jj}}, \xi'_{jj}, z'_h, \xi'_{jj} \right) \right. \right. \\ \left. \left. + (1 - p^{eu}(z, a)) (1 - p^{jj}(z, a)) (1 - p^b(\delta', a)) \tilde{H}_{a+1} \left(\tilde{n}'_h e^{z-z'_h} + e^{\epsilon'_a + \tilde{w}^C - (z'_h - z) - \pi}, \zeta, \tilde{w}^C - (z'_h - z) - \pi, z'_h \right) \right. \right. \\ \left. \left. \left. + (1 - p^{eu}(z, a)) (1 - p^{jj}(z, a)) p^b(\delta', a) \tilde{H}_{a+1} \left(\tilde{n}'_h e^{z-z'_h} + e^{\epsilon'_a + \xi}, \zeta, z'_h, \xi \right) \right] \middle| z \right] \right\}$$

$$\frac{\tilde{n}'_h}{1+r} + \tilde{c}_h = \tilde{\omega}$$

with the consumption policy functions given by

$$c_{u,a}(n, z, m) = e^z \tilde{c}_{u,a} \left(\frac{n + Be^z}{e^z}, z \right)$$

$$c_{h,a}(n, \zeta, z, \epsilon, w^C, m) = e^z \tilde{c}_{h,a} \left(\frac{n + e^{\epsilon+w^C}}{e^z}, \zeta, z, w^C - z \right)$$

Proof. The timing assumption that $a = 1$ when $m = 1$ implies that a is sufficient to keep track of m . We follow a guess-and-verify approach. The value functions are rewritten first. Some algebraic manipulation on the right-hand side of (4) yields:

$$\max_{c_u, n'_u \geq 0} \left\{ \frac{c_u^{1-\varphi}}{1-\varphi} + \beta \mathbb{E}_{\xi'_{ue}, z'_u, \epsilon'_a} \left[p^{ue}(z, a) H_{a+1}(n'_u, \xi'_{ue}, z'_u, \epsilon'_a, \xi'_{ue} + z'_u) + (1 - p^{ue}(z, a)) U_{a+1}(n'_u, z'_u) \middle| z \right] \right\}$$

$$\begin{aligned}
&= \max_{c_u, n'_u \geq 0} \left\{ \frac{(c_u/e^z)^{1-\varphi}}{1-\varphi} e^{(1-\varphi)z} + \beta \mathbb{E}_{\zeta'_{ue}, z'_u, \epsilon'_a} \left[e^{(1-\varphi)z'_u} \left[p^{ue}(z, a) \tilde{H}_{a+1} \left(\frac{n'_u + e^{\epsilon'_a + \zeta'_{ue} + z'_u}}{e^{z'_u}}, \zeta'_{ue}, z'_u, \zeta'_{ue} \right) + \dots \right. \right. \right. \\
&\quad \left. \left. \left. \dots + (1 - p^{ue}(z, a)) \tilde{U}_{a+1} \left(\frac{n'_u + B e^{z'_u}}{e^{z'_u}}, z'_u \right) \middle| z \right] \right] \right\} \\
&= e^{(1-\varphi)z} \max_{\tilde{c}_u, \tilde{n}'_u \geq 0} \left\{ \frac{\tilde{c}_u^{1-\varphi}}{1-\varphi} + \beta \mathbb{E}_{\zeta'_{ue}, z'_u, \epsilon'_a} \left[e^{(1-\varphi)(z'_u - z)} \left[p^{ue}(z, a) \tilde{H}_{a+1} \left(\tilde{n}'_u e^{z - z'_u} + e^{\epsilon'_a + \zeta'_{ue}}, \zeta'_{ue}, z'_u, \zeta'_{ue} \right) + \dots \right. \right. \right. \\
&\quad \left. \left. \left. \dots + (1 - p^{ue}(z, a)) \tilde{U}_{a+1} \left(\tilde{n}'_u e^{z - z'_u} + B, z'_u \right) \right] \right] \right\} \\
&= e^{(1-\varphi)z} \tilde{U}(\tilde{\omega}, z)
\end{aligned}$$

while the right-hand side of (6) becomes:

$$\begin{aligned}
&\max_{c_h, n'_h \geq 0} \left\{ \frac{c_h^{1-\varphi}}{1-\varphi} + \beta \mathbb{E}_{\zeta'_{jj}, z'_h, \epsilon'_a} \left[p^{eu}(z, a) U_{a+1}(n'_h, z'_h) + (1 - p^{eu}(z, a)) p^{jj}(z, a) H_{a+1}(n'_h, \zeta'_{jj}, z'_h, \epsilon'_a, \zeta'_{jj} + z'_h) \right. \right. \\
&\quad \left. \left. + (1 - p^{eu}(z, a)) (1 - p^{jj}(z, a)) (1 - p_b(\delta', a)) H_{a+1}(n'_h, \zeta, z'_h, \epsilon'_a, w^C - \pi) \right. \right. \\
&\quad \left. \left. + (1 - p^{eu}(z, a)) (1 - p^{jj}(z, a)) p_b(\delta', a) H_{a+1}(n'_h, \zeta, z'_h, \epsilon'_a, \zeta + z'_h) \middle| z \right] \right\} \\
&= \max_{c_h, n'_h \geq 0} \left\{ \frac{(c_h/e^z)^{1-\varphi}}{1-\varphi} e^{(1-\varphi)z} + \beta \mathbb{E}_{\zeta'_{jj}, z'_h, \epsilon'_a} \left[e^{(1-\varphi)z'_h} \left[p^{eu}(z, a) \tilde{U}_{a+1} \left(\frac{n'_h + B e^{z'_h}}{e^{z'_h}}, z'_h \right) + \dots \right. \right. \right. \\
&\quad \left. \left. \left. \dots + (1 - p^{eu}(z, a)) p^{jj}(z, a) \tilde{H}_{a+1} \left(\frac{n'_h + e^{\epsilon'_a + \zeta'_{jj} + z'_h}}{e^{z'_h}}, \zeta'_{jj}, z'_h, \zeta'_{jj} \right) + \dots \right. \right. \right. \\
&\quad \left. \left. \left. \dots + (1 - p^{eu}(z, a)) (1 - p^{jj}(z, a)) (1 - p_b(\delta', a)) \tilde{H}_{a+1} \left(\frac{n'_h + e^{\epsilon'_a + w^C - \pi}}{e^{z'_h}}, \zeta, z'_h, w^C - \pi - z'_h \right) + \dots \right. \right. \right. \\
&\quad \left. \left. \left. \dots + (1 - p^{eu}(z, a)) (1 - p^{jj}(z, a)) p_b(\delta', a) \tilde{H}_{a+1} \left(\frac{n'_h + e^{\epsilon'_a + \zeta + z'_h}}{e^{z'_h}}, \zeta, z'_h, \zeta \right) \right] \right] \right\} \\
&= e^{(1-\varphi)z} \max_{\tilde{c}_h, \tilde{n}'_h \geq 0} \left\{ \frac{\tilde{c}_h^{1-\varphi}}{1-\varphi} + \beta \mathbb{E}_{\zeta'_{jj}, z'_h, \epsilon'_a} \left[e^{(1-\varphi)(z'_h - z)} \left[p^{eu}(z, a) \tilde{U}_{a+1} \left(\tilde{n}'_h e^{z - z'_h} + B, z'_h \right) + \dots \right. \right. \right. \\
&\quad \left. \left. \left. \dots + (1 - p^{eu}(z, a)) p^{jj}(z, a) \tilde{H}_{a+1} \left(\tilde{n}'_h e^{z - z'_h} + e^{\epsilon'_a + \zeta'_{jj}}, \zeta'_{jj}, z'_h, \zeta'_{jj} \right) + \dots \right. \right. \right. \\
&\quad \left. \left. \left. \dots + (1 - p^{eu}(z, a)) (1 - p^{jj}(z, a)) (1 - p_b(\delta', a)) \tilde{H}_{a+1} \left(\tilde{n}'_h e^{z - z'_h} + e^{\epsilon'_a + w^C - (z'_h - z) - \pi}, \zeta, z'_h, w^C - (z'_h - z) - \pi \right) + \dots \right. \right. \right. \\
&\quad \left. \left. \left. \dots + (1 - p^{eu}(z, a)) (1 - p^{jj}(z, a)) p_b(\delta', a) \tilde{H}_{a+1} \left(\tilde{n}'_h e^{z - z'_h} + e^{\epsilon'_a + \zeta}, \zeta, z'_h, \zeta \right) \right] \right] \right\} \\
&= e^{(1-\varphi)z} \tilde{H}_a(\tilde{\omega}, \zeta, z, \tilde{w}^C)
\end{aligned}$$

Consequently, our guesses are correct. We now verify the budget constraints. Indeed:

$$\begin{aligned}
\frac{n'}{1+r} + c_u = n_u + B e^z &\iff \frac{n'/e^z}{1+r} + \frac{c_u}{e^z} = \frac{n_u}{e^z} + B \iff \frac{\tilde{n}'}{1+r} + \tilde{c}_u = \tilde{n}_u + B = \tilde{\omega} \\
\frac{n'}{1+r} + c_h = n_h + e^{\epsilon + w^C} &\iff \frac{n'/e^z}{1+r} + \frac{c_h}{e^z} = \frac{n_h}{e^z} + e^{\epsilon + w^C - z} \iff \frac{\tilde{n}'}{1+r} + \tilde{c}_h = \tilde{n}_h + e^{\epsilon + \tilde{w}^C} = \tilde{\omega}
\end{aligned}$$

As per the consumption policy functions, the reformulation procedure of the value functions indicate that if c_u^* is the consumption level that maximizes the right-hand side of (4) given states n, z , then c_u^*/e^z maximizes the right-hand side of the

recursion on \tilde{U}_a given the normalized states. The same logic applies for c_h^* . This completes the proof. \square

C Computational notes

We solve the transformed recursive problem in section B using the Endogenous Grid Method (EGM) proposed by [Carroll \(2006\)](#). Unlike alternative algorithms, EGM avoids root finding by constructing a grid for future endogenous variables over which policy functions are interpolated, thereby reducing computational burden. Given the presence of a no-borrowing constraint, the value functions and the consumption policy functions are approximated using cubic splines on their respective domains. We compute expectations via Gauss-Hermite quadrature.

The algorithm steps are as follows:

1. Initialize grids for $\tilde{\omega}$, ξ , and $\tilde{\omega}^C$. Let $G_{\tilde{\omega}}$ be the grid for $\tilde{\omega}$.
2. Solve the A -period's problem by setting consumption equal to cash-in-hand and the value functions equal to instantaneous utility:

$$U_a(\tilde{\omega}) = \frac{\tilde{\omega}^{1-\varphi}}{1-\varphi}, \quad c_{ua}(\tilde{\omega}) = \tilde{\omega}, \quad \tilde{n}'_{ua}(\tilde{\omega}) = 0$$

$$H_a(\tilde{\omega}, \xi, \tilde{\omega}^C) = \frac{\tilde{\omega}^{1-\varphi}}{1-\varphi}, \quad c_{ha}(\tilde{\omega}, \xi, \tilde{\omega}^C) = \tilde{\omega}, \quad \tilde{n}'_{ha}(\tilde{\omega}, \xi, \tilde{\omega}^C) = 0$$

Obtain the interpolation coefficients for these functions.

3. For $a < A$, fix a point of the grid for ξ , and $\tilde{\omega}^C$. Define an auxiliary grid $\tilde{n}^{vec} = [\tilde{n}'_1, \tilde{n}'_2, \dots, \tilde{n}'_K]$ with $\tilde{n}'_1 = 0$ and $\tilde{n}'_K = \tilde{\omega}_{max} - income$. The size of this grid is exactly the same as $G_{\tilde{\omega}}$.

- 3.1 For each \tilde{n}_i compute the expected marginal value function and consumption today:

$$B_{ua}(\tilde{n}') = \beta(1+r) \mathbb{E}_{\xi', \epsilon', v'} \left[e^{-\varphi(\gamma_u + v')} \left[p_a^{ue} c_{ha+1} \left(\tilde{n}' e^{-\gamma_u - v'} + e^{\epsilon' + \xi'}, \xi', \xi' \right)^{-\varphi} \right. \right. \\ \left. \left. + (1 - p_a^{ue}) c_{ua+1} \left(\tilde{n}' e^{-\gamma_u - v'} + B \right)^{-\varphi} \right] \right]$$

$$B_{ha}(\tilde{n}', \xi, \tilde{\omega}^C) = \beta(1+r) \mathbb{E}_{\epsilon', v', \xi'} \left[e^{-\varphi(\gamma_e + v')} \left[(1 - p_a^{eu}) c_{ha+1} \left(\tilde{n}' e^{-\gamma_e - v'} + e^{\epsilon' + \tilde{\omega}^C}, \xi', \tilde{\omega}^C \right)^{-\varphi} \right. \right. \\ \left. \left. + p_a^{eu} c_{ua+1} \left(\tilde{n}' e^{-\gamma_e - v'} + B \right) \right] \middle| \tilde{\omega}^C, \xi \right]$$

$$\tilde{c}_{ua}(\tilde{n}') = [B_{ua}(\tilde{n}')]^{-1/\varphi}$$

$$\tilde{c}_{ha}(\tilde{n}', \xi, \tilde{\omega}^C) = [B_{ha}(\tilde{n}', \xi, \tilde{\omega}^C)]^{-1/\varphi}$$

- 3.2 Compute the endogenous grid $\tilde{G}_{\tilde{\omega}}$ implied by:

$$\tilde{c}_{ua}(\tilde{n}') + \frac{\tilde{n}'}{1+r} = \tilde{\omega}'$$

$$\tilde{c}_{ha}(\tilde{n}', \xi, \tilde{\omega}^C) + \frac{\tilde{n}'}{1+r} = \tilde{\omega}'$$

In this way, the consumption policy function is defined on $\tilde{G}_{\tilde{\omega}}$, which is different from $G_{\tilde{\omega}}$.

- 3.3 Check that the no-borrowing constraint is satisfied. If not, set $\tilde{n} = 0$ and consumption equal to cash in hand. In other words, for all $\tilde{\omega} \in G_{\tilde{\omega}}$ and $\tilde{\omega} \leq \underline{\tilde{\omega}}$, with $\underline{\tilde{\omega}}$ defined as the first element of $G_{\tilde{\omega}}$ for which $\tilde{n}'_1 = 0$:

$$\tilde{c}_{ua}(\tilde{\omega}) = \tilde{\omega}, \quad \tilde{n}' = 0$$

$$\tilde{c}_{ha}(\tilde{\omega}, \xi, \tilde{\omega}^C) = \tilde{\omega}, \quad \tilde{n}' = 0$$

3.4 For all $\tilde{\omega} \in G_{\tilde{\omega}}$ and $\tilde{\omega} > \underline{\tilde{\omega}}$, interpolate the consumption policy function on the grid $\tilde{G}_{\tilde{\omega}}$. We obtain the consumption policies $\tilde{c}_{ua}(\tilde{\omega})$, $\tilde{c}_{ha}(\tilde{\omega}, \tilde{\xi}, \tilde{w}^C)$, which in turn allow us to compute savings:

$$\begin{aligned}\tilde{n}'_{ua}(\tilde{\omega}) &= (1+r)(\tilde{\omega} - \tilde{c}_{ua}(\tilde{\omega})) \\ \tilde{n}'_{ha}(\tilde{\omega}, \tilde{\xi}, \tilde{w}^C) &= (1+r)(\tilde{\omega} - \tilde{c}_{ha}(\tilde{\omega}, \tilde{\xi}, \tilde{w}^C))\end{aligned}$$

and value functions

$$\begin{aligned}U_a(\tilde{\omega}) &= \frac{\tilde{c}(\tilde{\omega})^{1-\varphi}}{1-\varphi} + \beta \mathbb{I}(a \leq A) \mathbb{E}_{\tilde{\xi}', \epsilon', \nu'} \left[e^{(1-\varphi)(\gamma_u + \nu')} \left[p_a^{ue} H_{a+1}(\tilde{n}'(\tilde{\omega})) e^{-\gamma_u - \nu'} + e^{\epsilon' + \tilde{\xi}'}, \tilde{\xi}', \tilde{\xi}' \right) + \dots \right. \\ &\quad \left. \dots + (1 - p_a^{ue}) U_{a+1}(\tilde{n}'(\tilde{\omega})) e^{-\gamma_u - \nu'} + B \right] \Big] \\ H_a(\tilde{\omega}, \tilde{\xi}, \tilde{w}^C) &= \frac{\tilde{c}(\tilde{\omega}, \tilde{\xi}, \tilde{w}^C)^{1-\varphi}}{1-\varphi} + \beta \mathbb{I}(a \leq A) \mathbb{E}_{\epsilon', \nu', \tilde{\xi}'} \left[e^{(1-\varphi)(\gamma_e + \nu')} \left[(1 - p_a^{eu}) H_{a+1}(\tilde{n}'(\tilde{\omega}, \tilde{\xi}, \tilde{w}^C)) e^{-\gamma_e - \nu'} + e^{\epsilon' + \tilde{w}^C}, \tilde{\xi}', \tilde{w}^C \right) + \dots \right. \\ &\quad \left. \dots + p_a^{eu} U_{a+1}(\tilde{n}'(\tilde{\omega}, \tilde{\xi}, \tilde{w}^C)) e^{-\gamma_e - \nu'} + B \right] \Big| \tilde{w}^C, \tilde{\xi} \Big]\end{aligned}$$

4. Iterate until $a = 1$. With the value functions found, compute the consumption equivalent.